Dear Peter Morse,

Thank you for handling our submission and for your recommendation. We answer point-by-point

1. Include photographs of the core in Supplementary Material.

Answer: We added core pictures as Supplementary Material (Figure S1) to section 4.2 *Cryolithology*.

2. Regarding the drill dimensions, just report the internal diameter, that is, the diameter of the extracted core.

Answer: The changed the according sentence in section 3.1 *Drilling and ground temperature measurements* as follows: "Core diameters were 109 mm for the upper parts and 73 mm for the lower ones."

3. Regarding Reviewer 2 comment for P4, L15, please indicate that cores were retrieved at intervals of 0.5 to 1.0 m, and the assembled cores were subsampled at XX intervals for analysis.

Answer: The changed the according sentence in section 3.1 *Drilling and ground temperature measurements* as follows: "The ice and permafrost deposits were sampled at intervals of about 0.5 to 1 m for hydrochemical and stable isotope analysis."

4. Regarding your model for pingo ice development: You base your interpretation on a segregated ice development model, with migration of water to the freezing front, but Reviewer 2 suggest the possibility of an intrusive ice origin. Mackay (1979, 1985, 1986) discusses a segregated-injection ice model that can switch between modes depending on rate of freezing. The air bubble morphology may tell you something more about the ice formation mechanism. Aligned bubbles are often related to segregated ice development, whereas irregular bubbles can be associated with freezing of bulk water. You should look into this, and determine if an injection origin is possible and consider if this may affect any interpretations.

Answer: We carefully read the recommended literature on ice types contributing to the massive pingo ice. We described irregularly distributed rounded bubbles and rather large ice crystals leading to high transparency (clear ice) where air bubbles were absent in the Fili pingo ice in section 4.2.1 *Core #9*, but were not able to observe bubble trains as described in Mackay (1979) as diagnostic for injection (intrusive) ice: "*Ice crystals in injection ice tend to be large (as much as 5 cm or more in diameter) and with bubble trains at right angles to the original freezing plane (GELL, 1976; MACKAY, 1962; MACKAY and STAGER, 1976; MULLER, 1959).*" This might be caused by our sampling approach of rather small core pieces proving only limited visibility of ice structures. We assume that parts of the studied Fili pingo massive ice formed by water injection. The presence of segregation ice is, however, also likely as the interplay of water pressure, overburden strength and freezing rate defines the prevalence of one or the other ice formation process (French *The Periglacial Environment*). This general understanding is mentioned in section 1 *Introduction*: "Hydraulic pingos occur where pressurised groundwater inflow from within or below permafrost freezes at the freezing front. Both processes result in a massive ice body composed of injection (intrusive) and/or segregation ice that heaves the surface and form conical elevations (Mackay, 1979)." While lacking proper observations of ice structures to solve the question whether injection and/or segregation ice mainly formed the Fili Pingo massive ice, we don't provide any discussion on this topic in the ms and base our interpretation of the freezing stages (open vs. closed system) solely on the stable water isotope data.

**Reviewer 1**
**Interactive comment on "Pingo development in Grøndalen, West Spitsbergen"**
**by Nikita Demidov et al.**
**Trevor Porter (Referee)**

The authors present stratigraphic profiles of solutes and water isotopes from pore ice of permafrost cores collected from the Fili pingo in West Spitsbergen, and of modern precipitation, tributaries, and a local spring to better constrain the origin of water in the pingo system. Based on the data, the authors deduce that the pingo is springfed, and that its evolution was characterised by several distinct periods of closed and semi-closed conditions, as evidenced by trends in the water isotope and solute data. They also use a Rayleigh isotope distillation model to show that the data diverge from a closed-system. I found the methods and interpretation were robust. The paper was well written, easy to follow and the topic is well suited for The Cryosphere. Below are several comments meant to help the authors improve the communication of their work, and address one uncertainty that is not discussed. Following these minor revisions I would recommend this paper for publication.
Answer: Thank you for your time and effort to review our manuscript. We appreciate your suggestions and answer them one-by-one. According changes in the manuscript are included in the revised version and referred in our replies.

**Major comments.**
I am intrigued by the vertical trends in the water isotope dataset. To a large extent I agree with the interpretation assuming the following conditions: core #9 was drilled exactly in the centroid of the ice body; pingo geometry is conical; and it is reasonable to assume the pingo grew equally on all sides. Largely these points are not discussed. Isotopic stratigraphy of pingo ice could show 'apparent' reversals if the coring angle was off-axis, or pingo growth was asymmetric. Perhaps the authors can comment on this uncertainty. Again, I am in agreement with the interpretation, but would appreciate if this issue of coring angle and pingo growth geometry could be discussed.

Answer: We agree that the interpretation of the vertical trends in the down-core profile strictly depends on the drilling position in the centroid of the massive ice body. Although the exact underground geometry of the massive ice has not been detected, we assume from the central drilling position at surface and concentric vertical drilling that the isotopic stratigraphy indeed represents the subsequent freezing stages of the pingo ice. Accordingly, we added in section 3.1 the following sentence: "The drilling position on top of the pingo was chosen in its center to assure that the centroid of the pingo ice body was captured in the core. The coring angle was held vertical." We further added the following sentence to section 5.2: "Assuming a conical geometry of the pingo ice body that grew equally to all sides, the chosen central drilling position on top of the pingo and the strictly vertical drilling allowed capturing subsequent freezing stages of the massive ice."

**Minor comments.**
Abstract. The final 2 sentences are largely unconnected to the research. Please finish the abstract with some kind of significance statement instead.

Answer: We changed the sentences as follows: "The presence of permafrost below the pingo ice body suggests that the talik is frozen and the water supply and pingo growth are terminated. The maximum thaw depth of the active layer reaching the top of the massive ice leads to its successive melt with crater development and makes the pingo extremely sensitive to further warming."

P2, L20-22. this sentence is too wordy, and confuses the message. please make it more concise.

Answer: We changed the sentence as follows: "They differentiate into group I pingos fed by sub-permafrost groundwater along geologic faults, group II pingos fed by artesian flow of migrating sub-

glacial groundwater mainly in river valley positions (*in sensu* Liestøl, 1977) and group III pingos (*in sensu* Yoshikawa and Harada, 1995). The latter are found in nearshore environments of post-glacial isostatic uplift and fed through small-scale discontinuities 'groundwater dikes' or taliks in aggrading permafrost within in marine deposits (Yoshikawa and Harada, 1995)."

P2, L24-26. please elaborate on why this is true.

Answer: The statement from Liestøl (1996) is still true and based on the scarcity of data from the inner structure of pingos due to lacking drilling or exposures except for the studies by referred in the manuscript in section 1. We added the following elaboration: "This is still valid due to the scarcity of data from the inner structure of pingos because of rarely undertaken drilling."

P3, L26-27. the description of core thickness in relation to different base level elevations is a bit confusing. Please clarify in simple terms.

Answer: We changed the sentence accordingly as follows: "The drilling of the Fili pingo in May 2017 started from the surface of central crater at 52.5 m asl and reached a depth of 11.5 m bs (core #9, 77.99355 °N, 14.66211 °E). The borehole was conserved and in April-May 2018 the drilling was continued in the same borehole down to a depth of 25 m bs"

P6, L17. The reported dD-d18O and d-dD slopes (6.7 and -0.2, respectively) are nearly identical to the slopes observed in modern precipitation. Fig. 3 indicates dD-d18O slope is 6.78, and based on the dD-d18O equation the d-dD slope can be calculated to -0.18 (or -0.2 if rounded to 1 decimal). My point is, your claim that the effects of freezing on the co-isotope slopes are not well supported by the data, since precipitation has these slopes.

Answer: To show difference in the *d*-δD data of the pingo massive ice (Figure 3c in the manuscript) and those of precipitation, we added here Figure R-1. Here is becomes obvious that the *d*-δD slope of precipitation is –0.06 and thus differs from those of the massive ice data. We therefore assume, that the co-isotope slopes of the massive ice as shown Figure 3 of the manuscript display the freezing effects during formation of the massive ice. The rather uncommon isotopic composition of modern precipitation are subject to a recent study by Skakun et al. (in review) where short-term variations in air mass trajectories are discussed to explain extrema in deuterium excess values.

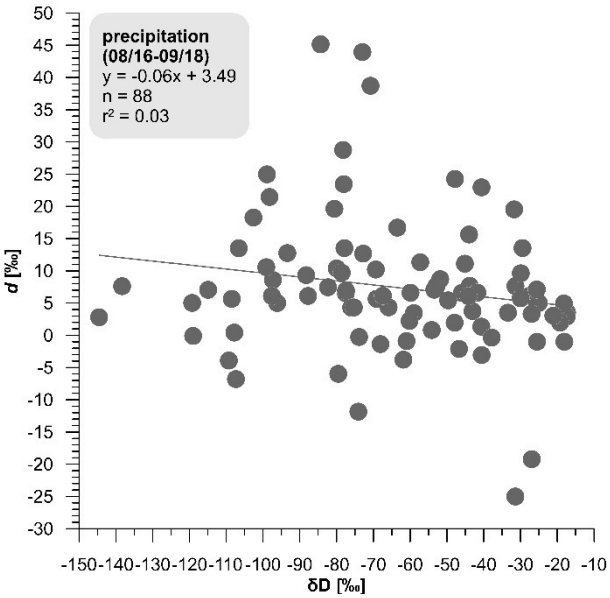


Figure R-1: Co-isotopic plot of *d* and δD in modern precipitation in Barentsburg not included in the paper.

Taking further into account the large scatter in precipitation amounting to about 18‰ in $\delta^{18}O$, to about 127 ‰ in δD (see Figure 3a and Table 1 in the manuscript) and to about 70 ‰ in *d* (see Figure R-1 above and Table 1 in the manuscript) if compared to those of the massive pingo ice the latter are distinctly smaller. Thus, if precipitation had been a major source for the pingo ice we would expect a much larger scatter in the isotopic composition.
Reference: Skakun et al.: Stable isotopic content of atmospheric precipitation and natural waters in the vicinity of Barentsburg (Svalbard), Ice and Snow (Лёд и Снег), in review.

P9, L19-20. it is unclear how the previous sentence justifies this conclusion. Please elaborate.

Answer: Based on literature data we assume a fast growth of the pingo massive ice. Accordingly, we changed the text as follows: “Estimations of pingo growth rate in Siberia and North America may reach values of order decimetres per year (Mackay, 1979; Chizhova and Vasil’chuk, 2018). Assuming a similar fast growth of the Fili pingo no or only little changes in isotopic composition of water source over the rather short period of pingo formation are likely. Thus, we assume the second controls on isotopic composition of the Fili pingo massive ice of less importance.”

P10, L12-13. If true, you may be able to calculate the rate of pore water recharge based on deviation from isotope distillation model.

Answer: The applied isotopic fractionation model does not allow calculating the admixture of water based on the deviation from the freezing line if the original isotopic composition of this additional source is unknown. There are two independent variables, and to find one, one needs to know the other, i.e., this problem is unsolvable.

P12, L10. …. valley evolution can already ‘be’ drawn.

Answer: Changed accordingly.

Figures. The font size and resolution of some of the figures is too low for publication, and in some cases it was difficult to interpret the figures as given. Please revise to conform to the publication standards of The Cryosphere.

Answer: To be changed accordingly in the final revision.

**Reviewer 2**
**Interactive comment on "Pingo development in Grøndalen, West Spitsbergen" by Nikita Demidov et al.**
**Go Iwahana (Referee)**

The paper "Pingo development in Grondalen, West Spitsbergen" by Demidov et al. presents very rare data set about internal structure and ice geochemistry of a pingo in West Spitsbergen. The paper discusses possible water sources and freezing conditions of the core ice, then growth history the pingos in target area. Especially, the cryolithological information with geochemistry of entire pingo core ice (with underlain sediment) is a paramount value for understanding frozen ground on Earth and other planets. This paper should be published ultimately with additional information after some clarifications of information provided and revision of discussion.

Answer: We are grateful for your time and effort to thoroughly review our manuscript. We appreciate your suggestions and answer them one-by-one. According changes in the manuscript are included in the revised version and referred in our replies.

**Major comments**
The title of paper is too broad, and it indicates overall study on pingo distribution and development history in Grondalen. However, the focus of this paper, to me, is unveiled internal structure of this particular pingo and interpretation of geochemistry of pingo ice and surrounding water. Could you revise the title so that reader can easily understand the contents of the paper more specifically?

Answer: We changed the title accordingly to "Geochemical signatures of pingo ice and its origin in Grøndalen, West Spitsbergen".

Discussion about water source of pingo ice is not clear mainly because the definition of precipitation is vague in the text. I encourage authors to reconstruct the discussion considering time and area of the precipitation and groundwater. I think the confusion came from the fact that the water sources of pingo ice and sources of groundwater (and river) are different concepts (groundwater can be a source of pingo ice, but the groundwater itself has its water sources.).

Answer: We differentiate generally three possible sources of water for the pingo ice: (1) atmospheric precipitation and its derivate as surface water, (2) sea water and (3) groundwater. Atmospheric waters feed the latter but due to subsurface turnover and interaction with rocks groundwater acquires geochemical signatures different from the atmospheric moisture. All three source have a sharply different composition from each other. The definition of precipitation in the manuscript solely refers to scarce modern precipitation stable isotope composition from 2016-17. Being limited to this we struggle to speculate on past precipitation, its past seasonality, precipitated area and groundwater recharge. In the course of our discussion we argue that atmospheric precipitation and surface waters are unlikely to be water sources that fed the pingo massive ice (see sections 5.1 and 5.2). Further elaborations on this topic are given in our replies to ref#2's specific minor comments below.

Section 5.3 should be rewritten and revise thoroughly to clearly present authors' discussion. Its paragraph structure does not match discussion flows. It was very hard to follow the logic of authors' idea and some statements don't sound to me as pointed in minor comments below.
Authors discussed hydrologic conditions and history of pingo growth comparing to Yoshikawa and Harada (1995) model; however, explanation, evidence and reasoning to suggestion of non-marine sedimentation are weak and discrepancy points between researches are unclear. This can be improved by describing more details about Yoshikawa and Harada (1995)'s development model and their reasoning if you intend to include this comparison in the conclusion. Please make it clear about

discrepancies and discussion in occurrence of sea regression at the target pingo location, timing of the regression, interpretation of sedimentation history at the site, and judgment of marine or non-marine sediment.

Answer: In this paper we do not touch the age of ice and deposits. We studied the geochemical signatures of the pingo ice and discussed based on this the possible water sources of the pingo ice. In the discussion section, we allowed ourselves to make cautious assumptions about the sequence of events in the formation of the pingo. The upper sequences of deposits drilled by well 11 and well 10 are probably processed by the river and spread marine deposits. River processing of sediments is visible on space images - meandering of the channel along the whole length of Grøndalen can be clearly traced. Desalinization is visible from the results of the water extraction analysis.

I think it is important to show photo of obtained cores for judgment of integrity, and also to capture cryolithologic properties of the target pingo as authors indicated as one of the purposes. Recovery of the entire massive ice core of a pingo is a dominant value of this study, however, cryolithological description and discussion of the obtained core is poor. Aim (1) can be more developed by comparing to other pingos on Spitsbergen (and in other regions?).

Answer: To our knowledge there are no comparable other records of internal pingo structures from Spitsbergen published. The Riverbed pingo in Adventdalen as referred in the manuscript (Yoshikawa, 1993) unfortunately was studied for other purposes, and it exposure in a distal position doesn't allow to comparison with the Fili pingo in Grøndalen. We agree with importance of photos of obtained cores. Following the recommendation of the editor, we added core pictures as Supplementary Material (Figure S1) to section 4.2.

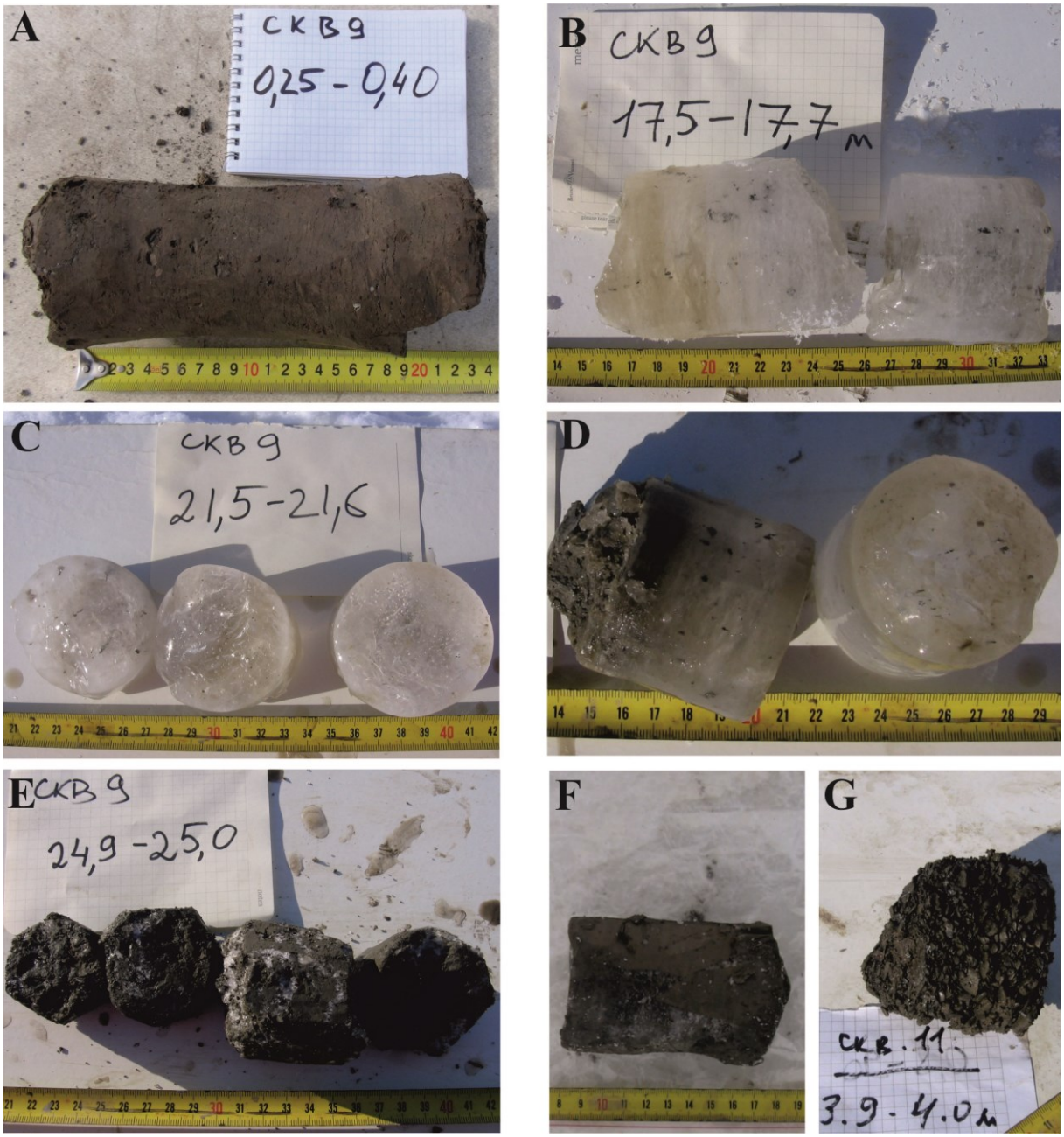


Figure R-2: Photos of obtained cores: A - gravelly loam at 0.25-0.4 m core #9 with wavy cryostructure, ice lenses up to 1 mm thick, B – transparent pingo ice containing dark silty flakes at 17.5-17.7 m core #9, C - crossection of pingo ice with dark silty flakes and air bubbles at 21.5-21.6 m core #9, D – boundary between massive ice and underlying sediments at 22.2 m core #9, E - dark clay with irregular reticulate cryostructures (ice lenses up to 5 mm thick) at 24.9-25.0 m core #9, F - ice-oversaturated deposits of core #10 at 4.95-5.2 m, G- gravelly sand with structureless cryostructure at 3.9-4.0 m core #11.

**Specific minor comments**

P2, first paragraph: please provide some references for these descriptions.

Answer: We agree with this comment and added the following reference to the manuscript:
van Everdingen, R.E.: Multi-language glossary of permafrost and related ground-ice terms (revised 2005), Boulder, USA: National Snow and Ice Data Center/World Data Center for Glaciology, 1998.

P2, L25: What are the unresolved questions relevant to this paper?

Answer: Following the recommendation from ref#1 we added the following sentence: ”This is still valid due to the scarcity of data from the inner structure of pingos because of rarely undertaken drilling.” The aims of the study follow in detail right afterward at the end of section 1.

P3, L23: I assume 5.5 m depth is the height difference between the crater rims and bottom, but it could mislead to be understood as water depth. What is the water depth? And did you drill through the ponding water (ice in May, right?) into the pingo core?

Answer: Following the recommendation from ref#2 we added the following sentences: “The maximum water depth of the lake was >1 m. At the point of drilling, the ice thickness was 0.15 m.”

P4, L3: Showing photos of cores will provide necessary information to judge stratigraphic integrity and possible contaminations.

Answer: See Figure R-2. We would leave it to the editor whether to include such photographs into the Supplementary Material of the paper or not. Following the recommendation of the editor, we added core pictures as Supplementary Material (Figure S1) to section 4.2.

P4, L4: “Drill diameters”, are these borehole’s or core’s diameters? What is the upper parts thickness?

Answer: Following the recommendation of the editor, we changed the sentence to: “Core diameters were 109 mm for the upper parts and 73 mm for the lower ones “

P4, L15-: Please provide information about subsampling interval for each measurement.

Answer: We added the sentence: “The ice and permafrost deposits were sampled at intervals of about 0.5 to 1 m for hydrochemical and stable isotope analysis.”

P4, L27: This sentence indicates water was extracted from sample cores, but the following sentence obviously tells the cores were dried first, then added DI water. Probably, the water extraction is after the drying and DI water adding procedure? Please clarify.

Answer: We agree with this comment and changed the text accordingly as follows: “Sedimentary permafrost samples of cores #9, #10 and #11 were dried and sieved at 1 mm at the analytical laboratory of RAE-S, Barentsburg. Afterwards about 20 g of the dry sediment were suspended in 100 ml de-ionised water and filtered through 0.45 µm nylon mesh within 3 minutes after stirring to estimate the ion content after water extraction.”

P5, L24: It is important to know how transparent and perfectly free from any inclusions (materials and bubbles) to understand formation of the massive ice. Could you show close-up photos of the ice? The next sentence mentions about 10% bubble inclusion in “single ice layers.” What does this mean (I guess it is a volume, though)? In my experience, even very bubble-rich ground ice contained are space about 5% of total ice volume.

Answer: We changed % to V%. Following the recommendation of the editor, we added core pictures as Supplementary Material (Figure S1) to section 4.2.

P5, L25: Is the dimension 1-2 -10-20mm thickness or length of the flakes? What is 0.5 %?

Answer: We added 1-2 to 10-20 mm long. We changed % to V%.

P5, L26: most air bubble should be rounded. Could you provide more information about the bubble shape? Oriented? Trained? Spherical other shape? What is 10 %? Again, photo is the best way to display this information.

Answer: We added following sentences. “In this particular layer and in all other layers of pingo massive ice bubbles are spherical and chaotic distributed. Most common are bubbles with diameter near 1 mm but some bubbles rich diameter up to 5 mm.“ See also Figure R-2.

P5, L27: “well defined lower contact to the basal deposits”, please provide photo and describe more about characteristics of the boundary ice and sediment.

Answer: We changed paragraph as follow: “The 25 m long core #9 drilled from the pingo top crater exposed cover and basal sedimentary horizons enclosing massive pingo ice. From 0 to 1.5 m bs gravelly loam was found, which is assumed origin from the pingo top and moved downslope by cryoturbation and solifluction. Below this redeposited cover layer from 1.5 to 12 m bs transparent massive ice without any inclusions is observed. Air bubble content reaches up to 10 V% in single ice layers. In this particular layer and in all other layers of pingo massive ice bubbles are spherical and chaotic distributed. Most common are bubbles with diameter near 1 mm but some bubbles rich diameter up to 5 mm. Between 12 and 22.2 m bs the pingo ice remains transparent, but contains layers with 1-2 to 10-20 mm long large dark silty flakes in subvertical orientation (up to 0.5 V%). Alternating layers include rounded air bubbles (up to 10 %). The total thickness of the massive pingo ice amounts to 20.7 m. Its lower contact to the basal deposits is well defined in the core. Massive pingo ice near the contact was not rich in air bubbles and had small admixture of previously mentioned dark silty flakes. The lower end of the massive pingo ice in our core #9 was found at depth of 22.2 m bs. Below down to a depth of 25 m bs dark clay with regular reticulate and irregular reticulate cryostructures (ice lenses 2 to 20 mm thick) was found in the core. At 23.8-24.3 m bs ice lenses were absent but 2-4 mm long lenses of black clay material were present. At 22.3-23.5 m bs and at 23.7-23.8 m bs layers of transparent ice without inclusions and without air bubbles were found.” See also Figure R-2.

P5, L27-28: “From 22.2 … is underlain by dark…” Ambiguous sentence. The layer 22.2-25m is the dark grey clay? Or within this layer the pingo ice is underlain by clay?

Answer: We changed sentences as follow. “The lower end of the massive pingo ice in our core #9 was found at depth of 22.2 m bs. Below down to a depth of 25 m bs dark clay with regular reticulate and irregular reticulate cryostructures (ice lenses 2 to 20 mm thick) was found in the core.”

P5, L29: Clear ice doesn’t necessarily mean segregation ice. The word “clear” is vague in this case. Do you mean just color, bubble-free or no inclusions?

Answer: We agree with this comment and specified the text accordingly as follows: “transparent ice without inclusions and without air bubbles”.

P6, L1: “top of the pingo” could indicate entire pingo-top crater. Do you mean top of the crater rim? Highest point?

Answer: We changed “top of the pingo” to “top of crater rim”.

P6, L2: What is “modern top soil” and “buried soil formation”? How did you differentiate them? “plant organic material” is terrestrial?

Answer: Modern soil - from the surface with living shrubs. The buried soil contains similar decomposed remains of vegetation. We changed sentence to: “The uppermost part from 0 to 2.5 m bs includes the modern top soil at 0 to 0.1 m bs with living shrub material and a buried soil formation at 0.25 to 0.4 m bs with decomposed similar shrub material.“

P6, L6: 1.2m (4.7 -5.9m) thick clear segregation ice? This is interesting data to understand the formation of this kind of frost mounds. Including photos of these cores is really helpful also for relevant researchers to understand development mechanism.

Answer: Please, see Figure R-2. Also taking in to account previous comment about “segregation ice” we changed the text as following: “From 2.5 to 12 m bs, the clay shows subhorizontal lenticular cryostructures up to 2 cm thick and includes ice-oversaturated deposits and ice with admixture of clay at 4.7- 5.9 m bs, at 6.65-7.05 m bs and at 8.2-8.6 m bs although the massive ice of the pingo was not reached. This ice and ice oversaturated deposits contain also sporadic gravel particles. In the layer 8.2-8.6 m ice contained up to 10 V% of spherical air bubbles with diameter near to 1 mm.“

P6, L11: “structure less cryostructure” can be displayed by photo.
Answer: See Figure R-2.

P7, L3: “sedimentary water extracts” indicates you measured extract water from the original samples. See my comment on P4, L27.

Answer: We changed the according method description in section 3.4 to make clear what sedimentary water extracts stands for as follows: “Sedimentary permafrost samples of cores #9, #10 and #11 were dried and sieved at 1 mm at the analytical laboratory of RAE-S, Barentsburg. Afterwards about 20 g of the dry sediment were suspended in 100 ml de-ionised water and filtered through 0.45 µm nylon mesh within 3 minutes after stirring to estimate the ion content after water extraction.”

P7, 23-25: Why this points to the non-marine origin. Could you explain this in detail? This relates to one of your important conclusions.

Answer: The section 4.4.2 solely presents the results that are further discussed in discussion section 5. Therefore, no interpretation of the data is given here. We deleted last part of the sentence “pointing to the non-marine origin of the deposits” from the text.

P9, L2: “on the mounts of valley sides…”?

Answer: We agree with this comment and changed the term accordingly to: “Glaciers on the mounts surrounding the valley”.

P9, L10: Is the source water exclusively from sub-glacial melt? Is there any contribution from rain or snow melt?

Answer: This is discussed earlier in section 5.1 as follows: “Precipitation and surface waters in Grøndalen have lower ion contents and different composition if compared to the pingo massive ice (Table 2), which also excludes these sources as the main ones for the pingos of Grøndalen.” And further in section 5.2 as follows: “This is much lower than the modern mean annual precipitation values in the Barentsburg region with –9.0±4.2 ‰ in $\delta^{18}O$ and –64±30 ‰ in δD, and closer to mean

values of the Grøn River and its tributaries with about –11.7±0.3 ‰ in $\delta^{18}O$ and –78±3 ‰ in δD (Table 1). Thus, if precipitation was the main source of the massive ice, its onset took place during a colder period than today. More likely, the underground water sources feeding spring near the pingo was the same source for the massive pingo ice." We also point out that underground water is currently isolated from surface water due to permafrost.

P9, L19-20: I could not understand the logic of this sentence and the previous explanation.

Answer: Based on literature data we assume a fast growth of the pingo massive ice. Accordingly, we changed the text as follows: "Estimations of pingo growth rate in Siberia and North America may reach values of order decimetres per year (Mackay, 1979; Chizhova and Vasil'chuk, 2018). Assuming a similar fast growth of the Fili pingo no or only little changes in isotopic composition of water source over the rather short period of pingo formation are likely. Thus, we assume the second controls on isotopic composition of the Fili pingo massive ice of less importance."

P9, L21: Do you have any information of discussion about how stable or variant geochemistry of the spring water seasonally and inter-annually?

Answer: Unfortunately, we have yet only single point observations. The only data available is included in our study. Therefore, any temporal variability of the spring water stable isotope composition remains unknown. We can only point out that in spring and summer 2019 we observed the water coming from this spring and that organoleptic property of water was the same.

P10, L3-5: As you discussed earlier, the source water came from glacier melt in the upper area of the valley. Past precipitation (rain and snow) in the ground water source area would also be a probable water source for the pingo ice? "precipitation" in this paper should be well-defined because there are many types depending on time-scale, season, and precipitated area (if you discuss about groundwater source, precipitation in the recharge area might be different from that in your sampling area of precipitation and river data.).

Answer: As already stated above to reply on comment P9, L10, precipitation and surface waters are unlikely to be the water source feeding the growing pingo ice. This is given in section 5.1 as follows: "Precipitation and surface waters in Grøndalen have lower ion contents and different composition if compared to the pingo massive ice (Table 2), which also excludes these sources as the main ones for the pingos of Grøndalen." And further in section 5.2 as follows: "This is much lower than the modern mean annual precipitation values in the Barentsburg region with –9.0±4.2 ‰ in $\delta^{18}O$ and –64±30 ‰ in δD, and closer to mean values of the Grøn River and its tributaries with about –11.7±0.3 ‰ in $\delta^{18}O$ and –78±3 ‰ in δD (Table 1). Thus, if precipitation was the main source of the massive ice, its onset took place during a colder period than today. More likely, the underground water sources feeding spring near the pingo was the same source for the massive pingo ice."
Please, find also our reply to the comment of ref#1 on precipitation data, P6, L17:
To show difference in the *d*-δD data of the pingo massive ice (Figure 3c in the manuscript) and those of precipitation, we added here Figure R-1. Here is becomes obvious that the *d*-δD slope of precipitation is –0.06 and thus differs from those of the massive ice data. We therefore assume, that the co-isotope slopes of the massive ice as shown Figure 3 of the manuscript display the freezing effects during formation of the massive ice. The rather uncommon isotopic composition of modern precipitation are subject to a recent study by Skakun et al. (in review) where short-term variations in air mass trajectories are discussed to explain extrema in deuterium excess values.

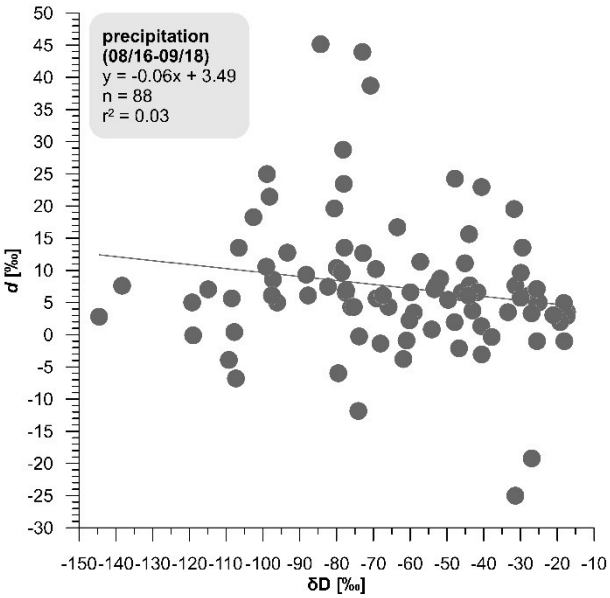

Figure R-1: Co-isotopic plot of *d* and δD in modern precipitation in Barentsburg not included in the paper.

Taking further into account the large scatter in precipitation amounting to about 18‰ in $\delta^{18}O$, to about 127 ‰ in δD (see Figure 3a and Table 1 in the manuscript) and to about 70 ‰ in *d* (see Figure R-1 above and Table 1 in the manuscript) if compared to those of the massive pingo ice the latter are distinctly smaller. Thus, if precipitation would have been a major source for the pingo ice we would expect a much larger scatter in the isotopic composition.
Reference: Skakun et al.: Stable isotopic content of atmospheric precipitation and natural waters in the vicinity of Barentsburg (Svalbard) in 2016-2017, Ice and Snow (Лёд и Снег), in review.

The only data available to us yet is modern precipitation stable isotope composition from 2016-17. Being limited to this we struggle to speculate on past precipitation, its seasonality and precipitated area.

P11, 10-11: "Generally…" I cannot understand this sentence. Please revise it and provide some references.

Answer: We deleted accordingly this sentence and the previous one from the text.

P11, L22-24: This is a long sentence and it's hard to understand. It is not clear to me why authors need to state this. It is better to bring comparable observations of internal structure of other pingos.

Answer: To our knowledge there are no comparable other records of internal pingo structures from Spitsbergen published. The Riverbed pingo in Adventdalen as referred here unfortunately was studied for other purposes, and it exposure in a distal position doesn't allow to comparison with the Fili pingo in Grøndalen. Because pingos are to our understanding features mainly controlled by local hydrological and morphological conditions any comparison of the Fili pingo record to those from other arctic regions seems inappropriate. To clarify our thought we changed the sentence as following: The Riverbed pingo in Adventdalen as referred in (Matsuoka et al., 2004) unfortunately was studied for other purposes, and it exposure in a distal position doesn't allow to comparison with the Fili pingo in Grøndalen, where borehole in the centre of mound exhibits the entire massive ice.

P11, L28-30: Hard to understand. Please explain about "step-wise massive ice growth".

Answer: We deleted accordingly 'stepwise' from this sentence.

P11, L33: I could not understand this logic. Do you mean the massive ice started to grow when freezing front reached at 15m depth and most of the upper sediment layer was lost by solifluction?

Answer: The thickness of the massive ice (20.7 m) exceeds the height of the pingo of 9.5 m, which is explained by massive ice growth when the ongoing subsurface freezing pushed the previously formed ice and cover deposits upward. The latter moved subsequently from the pingo top down-slope by solifluction. Thus, the 9.5 m amplitude of surface uplift seen in the modern stage of pingo evolution became less than the 20.7 m thickness of the massive ice.

P12, L10-12: I don't find the first half of this sentence is general fact. The second half seems to be too obvious to state.

Answer: We deleted accordingly this sentence.

P12, L12-13: Please explain why Yoshikawa and Harada (1995) concluded this.

Answer: The original paper there is no explanation or more detailed elaboration given. The relevant section reads as follows: "Pingos in Grøndallen and at the mouth of the Reindalen are situated about 50 m above sea level. This is the same level as the maximum elevation of Holocene marine deposits. The pingo overburden is composed of marine material. There are several generations of pingos that started growth quickly after retreat of the sea. They do not have non-marine sediments over the marine deposits as does the area surrounding the pingos. These pingos are considered former group III pingos."

P12, L16: Is the presence of gravelly sand and loam the only reason for non-marine deposit? It is unclear if authors suggestions are contradicting to marine deposits only or pingo growth after sea regression as referred by Yoshikawa and Harada (1995).

Answer: The statement of Yoshikawa and Harada (1995) is shown above. To our understanding this statements claims pingo growth within marine deposits as characteristic for group III pingos which is unfortunately not based on specific data from Grøndalen in the paper by Yoshikawa and Harada (1995). Besides the granulometric properties of the Grøndalen valley deposits also the sedimentary water extract hydrochemistry from our study as described in sections 4.4.2 and 4.4.3 and discussed in section 5.1 clearly show the terrestrial (non-marine, or reworked marine) origin of the valley deposits of Grøndalen in which the pingos formed. Thus, our suggestions do not contradict pingo growth after deglaciation and sea level regression, but the marine character of the deposits in which the Grøndalen pingos formed.

P12, L18: This sentence doesn't sound to me because heaving amount that forms current pingo height could advance any moment of freezing of intruding water. Are you assuming intrusion of groundwater into the pingo bottom started when the ground was frozen down to 15m? Is there any possibility the intrusion happened earlier, and advance of entire ground freezing and intrusive ice core development happen at the same time?

Answer: Here we rely on the conventional mechanism of formation of swelling hillock by means of moisture migration to the freezing front (Kudryavtsev V.A. (ed.): Obshcheye Merzlotovedeniye (Geocryology). Moscow, Izdatelstvo Moskovskogo Universiteta, 1978 (in Russian)). According to this mechanism, the lower boundary of the ice core will correspond to the position of the freezing front at which the ice formation began.

P12, L34: Please explain and define “warm-based” and “cold-based” glaciers.

Answer: We use this commonly used in glaciology terms. For example in (Bennet M.R. and Glasser N.F.: Glacial geology: ice sheets and landforms. Oxford, Wiley-Blackwell. 385 pp.,2009) they are explained as following. Cold-based glaciers are glaciers which are frozen to their beds and no meltwater is present at the ice-bed interface. In contrast, in warm-based glaciers basal ice is constantly melting and the ice-bed interface is therefore lubricated with meltwater.

P13, L2: What is “rare locations”?

Answer: We agree with this comment and deleted accordingly “at rare locations” from this sentence.

P13, L10: active layer depth -> active layer thickness, or in this case maximum thaw depth would be suitable.

Answer: We agree with this comment and changed the term accordingly to: “maximum thaw depth”.

P13, L11: “fast” degradation -> temporal degradation rate are not discussed in this paper. Authors should provide evidence of ongoing fast degradation and strong solifluction (against degraded in the past but stabilized) if they want to conclude this.

Answer: In our text it is written “The maximum thaw depth of 1.5 m in September 2018 reached the uppermost massive ice, which indicates the ongoing fast degradation of the pingo. This is further seen in the crater lake on top of the pingo and strong solifluction that removes cover deposits downslope.“ It means that from temperature measurements in the borehole we know that zero degrees isotherm reaches upper boundary off massive ice in the end of warm season leading to irrevocable melting of ice and crater deepening. In addition to temperature measurements it must be mentioned that upper part of 3 m long plastic drive pipe which had been inserted to the borehole to prevent water propagation to the borehole from active later after end of first stage of drilling in May 2017 was found in April 2018 declinated on 0.5 m in the direction of solifluction removal.

P13, L18: It was hard to understand this sentence. Characteristics of what? Non-marine character of the pingo deposits indicate fault-related groundwater discharge and ground-water origin from warm-based glaciers are unlikely? But I couldn’t understand why.

Answer: Changed accordingly to: “In the Fili pingo record of Grøndalen we concurrently identified pingo-formation characteristics such as fault-related groundwater discharge (typical for group I pingos) and ground-water origin from warm-based glaciers (typical for group II pingos). The proposed pingo formation in Grøndalen is connected to epigenetic refreezing of marine deposits (typical for group III pingos) but not immediately after sea regression due to the reworking of marine sediments (or nonmarine origin of sediments) seen in deposits surrounding the Grøndalen pingos.”

P13, L22-24: This sentence needs to be rephrased or edited.

Answer: Changed accordingly to: “The origin and distribution of pingos in Grøndalen depends on the complex interaction of hydrogeological conditions and sea level, glaciers and permafrost dynamics superimposed by climate variability over time. The latter may be typical for vast archipelago and makes investigation of pingos important for understanding key stages of cryosphere evolution of Spitsbergen.“

Table 1: What the “v” indicates?

Answer: The “v” in two places in Table 1 is an artefact from previous draft versions of the manuscript. It is replaced by the minus symbol “—“ in the revised manuscript.

Fig 1: Provide contour lines information.

Answer: Contour lines information is shown in revised figure.

Fig 1: Could you add information of geological faults location/direction?

Answer: Geological faults are shown in the revised figure.

Fig 2: Why the sample intervals of stable isotopes and ions are so different, especially in the unit II?

Answer: We tried to take samples every 0.5 m. The irregularity of the samples analysed is due to the loss of samples during drilling, storage and analysis.

Fig 4 (a): One more value should be in the y-axis.

Answer: Changed accordingly in the revised Figure 4.

Fig 2-5: Use different symbols for different components in same figures so that readers can distinguish them in black&white printouts.

Answer: For clarity of the figures and to better distinguish single data points and curves, we’d prefer to present our data in colour plots. We’d leave the decision with the handling editor and the production manager of “The Cryophere” whether to show black-and-white compatible or colour figures in the final version.

Fig 6: Please revise this image so that it can display difference between authors’ and Yoshikawa & Harada (1995) development models.

Answer: Our figure reflects the specific situation in the Grøndalen Valley. Here, the retreat of the sea, the onset of freezing, and the migration of moisture from the bottom melting of glaciers through the underground aquifer appear, which was not mentioned in the article by Yoshikawa & Harada (1995).

# Geochemical signatures of pingo ice and its origin in Grøndalen, West Spitsbergen

Nikita Demidov[1], Sebastian Wetterich[2], Sergey Verkulich[1], Aleksey Ekaykin[1,3], Hanno Meyer[2], Mikhail Anisimov[1,3], Lutz Schirrmeister[2], Vasily Demidov[1], Andrew J. Hodson[4, 5]

[1]Arctic and Antarctic Research Institute, Bering St. 38, 199397 St. Petersburg, Russia

[2]Alfred Wegener Institute Helmholtz Center for Polar and Marine Research, Telegrafenberg A45, D-14473 Potsdam, Germany

[3]St. Petersburg State University, 10th Line 33-35, 199178 St. Petersburg, Russia

[4]University Centre in Svalbard, N-9171 Longyearbyen, Norway

[5]Western Norway University of Applied Sciences, Røyrgata 6, N-6856 Sogndal, Norway

*Correspondence to*: Nikita Demidov (nikdemidov@mail.ru)

**Abstract.** Pingos are common features in permafrost regions that form by subsurface massive-ice aggradation and create hill-like landforms. Pingos on Spitsbergen have been previously studied to explore their structure, formation timing, connection to springs as well as their role in post-glacial landform evolution. However, detailed hydrochemical and stable-isotope studies of massive ice samples recovered by drilling has yet to be used to study the origin and freezing conditions in pingos. Our core record of 20.7 m thick massive pingo ice from Grøndalen differentiates into four units: two characterised by decreasing $\delta^{18}O$ and δD and increasing *d* (units I and III), and two others show the opposite trend (units II and IV). These delineate changes between episodes of closed-system freezing with only slight recharge inversions of the water reservoir, and more complicated episodes of groundwater freezing under semi-closed conditions when the reservoir got recharged. The water source for pingo formation shows similarity to spring water data from the valley with prevalent $Na^+$ and $HCO_3^-$ ions. The sub-permafrost groundwater originates from subglacial meltwater that most probably followed the fault structures of Grøndalen and Bøhmdalen. The p~~P~~resence of permafrost ~~under~~below the pingo ice body ~~of pingo~~ suggests that the talik is frozen, and ~~termination of~~ the water supply and pingo growth are terminated. The m~~M~~aximum thaw depth of the active layer reaching the top of the massive ice leads to its successive melt with crater development and makes the pingo extremely sensitive to further~~climate~~ warming. ~~Today the pingo of Grøndalen is relict and degrading due to warming surface temperatures. The state of pingos on Spitsbergen depends on complex interaction of climate, permafrost and groundwater hydrology conditions, and is thus highly sensitive to climate warming.~~

## 1 Introduction

Pingos are widespread landforms that occur within the permafrost zone of the Earth (Grosse and Jones, 2011) and likely on Mars (Burr et al., 2009). The distribution of pingos is closely linked to permafrost history, underground hydrology and climate conditions. Two pingo types are commonly distinguished, which are (1) hydrostatic (closed) system and (2) hydraulic (open) system pingos (van Everdingen, 1998). Hydrostatic pingos form when a distinct volume of pore water in water-saturated deposits expulses towards the freezing front and freezes. Hydraulic pingos occur where pressurised groundwater inflow from within or below permafrost freezes at the freezing front. Both processes result in a massive ice body composed of injection (intrusive) and/or segregation ice that heaves the surface and form conical elevations (Mackay, 1979). Pingos have a characteristic elliptical to circular planar shape reaching diameters of up to several hundred meters and heights of up to several dozen meters.

Pingos are rather well studied in Alaska and Canada in terms of formation (e.g. Mackay, 1962), structure (e.g. Yoshikawa et al., 2006) and distribution (e.g. Jones et al., 2012). Pingo growth and decay rates, pingo age, and past distribution of those landforms have been used for the reconstruction of past periglacial landscape conditions (e.g. Mackay, 1986). Pingo ice and sedimentary inventories were investigated and furthermore employed in palaeoenvironmental reconstructions in the Mackenzie Delta in Canada (Hyvärinen and Ritchie, 1975), on Seward Peninsula in Alaska (Wetterich et al., 2012; Palagushkina et al., 2017), in Siberia (Ulrich et al. 2017; Chizhova and Vasil'chuk, 2018; Wetterich et al., 2018), where they are called 'bulgunniakhs', and in northern Mongolia (Yoshikawa et al., 2013; Ishikawa and Yamkhin, 2016).

Pingos on Spitsbergen (76 identified pingos by Hjelle, 1993) are commonly attributed to open-system conditions (Liestøl, 1977), and have previously been studied by geophysical techniques (e.g. Ross et al., 2005; Rossi et al., 2018) and combined chemical and physical investigation of the properties of pingo ice (e.g. Yoshikawa, 1993; Yoshikawa and Harada, 1995). Unlike in other permafrost regions, stable isotope properties of the pingo ice were rarely studied on Spitsbergen (Matsuoka et al., 2004).

Yoshikawa and Harada (1995) proposed three formation mechanisms for open-system pingos on Spitsbergen. ~~They differentiate into pingos fed by sub-permafrost groundwater along geologic faults (group I), pingos fed by artesian flow of migrating sub-glacial groundwater mainly in river valley positions (*in sensu* Liestøl, 1977, group II) and pingos, which are found in nearshore environments of post-glacial isostatic uplift and fed through small-scale discontinuities 'groundwater dikes' (*in sensu* Yoshikawa and Harada, 1995, group III) or taliks in permafrost that aggrades in marine deposits.~~ They differentiate into group I pingos fed by sub-permafrost groundwater along geologic faults, group II pingos fed by artesian flow of migrating sub-glacial groundwater mainly in river valley positions (*in sensu* Liestøl, 1977) and group III pingos (*in sensu* Yoshikawa and Harada, 1995). The latter are found in nearshore environments of post-glacial isostatic uplift and fed through small-scale discontinuities 'groundwater dikes' or taliks in aggrading permafrost within in marine deposits (Yoshikawa and Harada, 1995).

Yoshikawa and Harada (1995) regard the pingos of the Grøndalen as ancient group III pingos, which formed in Holocene marine sediments quickly after sea regression. However, as Liestøl (1996) recognised 'In connection with formation of pingos there are a great many unsolved questions. Drillings and temperature measurements through the pingo mound and also through the surrounding permafrost are needed before the problems can be better understood'. This is still valid due to the scarcity of

data from the inner structure of pingos because of rarely undertaken drilling. To shed light on the Grøndalen pingo formation in comparison to other pingo records from Spitsbergen, we here present the stable isotope and hydrochemical inventories of an entirely cored pingo in Grøndalen near Barentsburg (West Spitsbergen, Fig. 1). Additional data for consideration of postglacial landform evolution in the Grøndalen were obtained from neighbouring sedimentary cores. The aims of our study are (1) to capture the morphometric, cryolithologic and thermic properties of the Grøndalen pingo in comparison to other pingos on Spitsbergen and (2) to reconstruct the formation conditions of the pingo massive ice by applying stable isotope and hydrochemical approaches.

## 2 Study area

The Grøndalen study area on the western coast of Nordenskiöld Land (West Spitsbergen) is in about 10 km distance south-east of Barentsburg in whose vicinity the Russian Scientific Arctic Expedition on Spitsbergen Archipelago (RAE-S), maintains ground temperature and active-layer monitoring sites of the Global Terrestrial Network for Permafrost (GTN-P) and the Circumpolar Active Layer Monitoring (CALM) programs (Demidov et al., 2016; Christiansen et al., 2019). The Grøndalen is a trough valley in bedrock of Middle Jurassic–Palaeogene argillite and sandstone (Geological map Svalbard, 1991). Late Pleistocene and Holocene deposits in the lower part of Grøndalen reach more than 20 m thickness and likely represent sedimentation since at least the last glacial maximum (Verkulich et al., 2018). The mountains surrounding the valley reach up to 700-800 m above sea level (asl). The Grøn River is fed by many tributaries, which collect meltwater discharge from small hanging glaciers. In the upper valley part occur two larger glaciers, Tavlebreen and Passfjellbreen, as well as their terminal moraines.

The meteorological station in Barentsburg (WMO station #20107) at 75 m asl recorded a mean annual air temperature of –2.2 °C and a mean annual precipitation of 849 mm for 2016-2017. The ground temperatures reach –2.37 °C at 15 m depth below surface (bs) and the active layer thickness at the CALM site (3 km north of Barentsburg) measured in the end of September 2016 varied from 1.15 to 2.60 m with an average of 1.56 m (Demidov et al., 2016). Permafrost thickness in Barentsburg area varies along with morphology from 8-10 m near the seashore up to 300-450 m in the mountain and upland areas. According to measurements in the central part of Grøndalen the mean annual ground temperature amounts to -3.56 °C at depth of 15 m (borehole #8). ~~Thus, the permafrost thickness probably exceeds 100 m below the valley surface.~~

In the central part of Grøndalen, a group of seven pingos occurs reaching diameters of 150 to 300 m and heights above their surroundings from 6.5 to 12.5 m (Fig. 1b). They are informally named as follows (west to east on Fig. 1b): Nori, Ori, Dori, Fili, Kili, Oin, Gloin after John R.R. Tolkien (1954-1955). The pingo Fili of 9.5 m maximum height (56 m asl) was chosen for drilling. It shows a clearly defined uppermost water-filled degradation crater of 5.5 m depth. The maximum water depth of the lake was >1 m. At the point of drilling, the ice thickness was 0.15 m. The drilled Fili pingo is to the northeast and the southwest connected to Dori pingo and Kili pingo (Fig. 1b) and its slope shows radial dilation cracks.

## 3 Materials and methods

### 3.1 Drilling and ground temperature measurements

~~The drilling of the pingo performed in May 2017 reached a depth of 11.5 m bs (core #9, starting from 52.5 m asl, 77.99355 °N, 14.66211 °E), and was continued down to 25 m bs in April-May 2018.~~ The drilling of the Fili pingo in May 2017 started from the surface of central crater at 52.5 m asl and reached a depth of 11.5 m bs (core #9, 77.99355 °N, 14.66211 °E). The borehole was conserved and in April-May 2018 the drilling was continued in the same borehole down to a depth of 25 m bs. The drilling position on top of the pingo was chosen in its cent~~e~~re to assure that the centroid of the pingo ice body was captured in the core. The coring angle was held vertical. Additional cores were drilled on the pingo top reaching a depth of 12 m (core #10, from 56 m asl, 77.99332 °N, 14.66114 °E) and in the pingo surroundings reaching a depth of 6 m (core #11, from 47 m asl, 77.99531 °N, 14.66538 °E). Continuous temperature measurements in borehole #9 on Fili pingo were installed on 15 May 2018 using a 15-m long Geo Precision logger chain (M-Log5W cable) equipped with sensors every 0.75 m.

The cores were obtained with a portable gasoline-powered rotary drilling rig (UKB 12/25, Vorovskiy Machine Factory, Ekaterinburg, Russia) that allows performing operations without impact on the ecosystem. The device uses no drilling fluid, and relies on maintaining the frozen condition of the core for stratigraphic integrity and to prevent downhole contamination of the biogenic and sedimentological characteristics of the core. Core~~Drill~~ ~~barrels~~outer ~~-~~diameters were ~~112 -~~109 mm for the upper parts and ~~76 -~~73 mm for the lower ones. ~~The barrels wall thickness is 3 mm.~~ The core pieces were lifted to the surface every 30–50 cm. After documentation and cryolithological description (French and Shur, 2010) core pieces were sealed. The ice and permafrost deposits were sampled at intervals of about ~~one half~~0.5 to 1 ~~one meter~~m for hydrochemical and stable isotope analysis. Ice samples were kept frozen for transportation while sediment samples were kept unfrozen.

To obtain spring water samples at the foot of the Oin pingo near the right bank of the Grøn River drilling was performed through ca. 1 m of ice to pressurised water beneath an ice blister that formed at the spring source on 20 April 2018. Samples were then taken of the water discharging through the 5 cm drill hole.

### 3.2 Mapping

The topographic mapping on 21 August 2018 covered an area of 0.25 $km^2$ using Global Navigation Satellite System (GNSS) Sokkia GRX2 devices and an Archer 2 base station. The obtained coordinates have planar accuracy of 1.5 cm and altitude accuracy of 2.5 cm.

### 3.3 Stable water isotopes

The concentration of water isotopes (δD and $\delta^{18}O$) was measured at Climate and Environmental Research Laboratory (CERL, AARI St. Petersburg, Russia) using a Picarro L2120-*i*analyzer. The working standard (SPB-2), measured after every five samples, was made of the distilled St. Petersburg tap water and calibrated against the IAEA standards VSMOW-2, GISP and SLAP-2. The reproducibility of results defined by re-measurements of randomly chosen samples was 0.08 ‰ for $\delta^{18}O$ and 0.4

‰ for δD, which is two orders of magnitude less than the common natural variability of the pingo ice isotopic composition and thus satisfactory for the purposes of the study. Additional samples from Grøndalen spring water were collected as unfiltered 20 ml aliquots in a screw-top HDPE bottle and analysed 6 times using a Picarro V 1102-I and a 2.5 µl injection volume with a precision error of 0.1 ‰ for $\delta^{18}O$ and 0.3 ‰ for δD. The $\delta^{18}O$ and δD values are given as per mil (‰) difference to the Vienna Standard Mean Ocean Water (VSMOW) standard. The deuterium excess ($d$) is calculated as $d = \delta D - 8\delta^{18}O$ (Dansgaard, 1964).

### 3.4 Hydrochemistry

Sedimentary permafrost samples of cores #9, #10 and #11 were dried and sieved at 1 mm at the analytical laboratory of RAE-S, Barentsburg. Afterwards about 20 g of the dry sediment were suspended in 100 ml de-ionised water and filtered through 0.45 µm nylon mesh within 3 minutes after stirring to estimate the ion content after water extraction.~~The ion content of sedimentary permafrost samples of cores #9, #10 and #11 was estimated after water extraction at the analytical laboratory of RAE-S, Barentsburg. The material was dried and sieved at 1 mm. About 20 g of the sediment were suspended in 100 ml de-ionised water and filtered through 0.45 µm nylon mesh within 3 minutes after stirring.~~ Electrical conductivity (EC measured in µS $cm^{-1}$) and pH values were estimated with Mettler Toledo Seven Compact S 220. EC values were transformed automatically by the instrument in to general ion content values given as mg $l^{-1}$. Major anions and cations in the water extracts were analysed by ion chromatography (Shimadzu LC-20 Prominence) equipped with the conductometric detector Shimadzu CDD-10AVvp and ion exchange columns for anions (Phenomenex Star-ion A300) and for cations (Shodex ICYS-50). Likewise melted pingo ice samples from core #9, snow and Grøn River water were analysed for pH, EC and ion composition after filtration through 0.45 µm nylon mesh. Spring water analysis of anions $Cl^-$, $NO_3^-$, $PO_4^{3-}$ and $SO_4^{2-}$ employed a Dionex ICS90 ion chromatography module calibrated in the range 0 – 2 mg $l^{-1}$ for $NO_3^-$ and $PO_4^{3-}$ and in the range 0 – 50 mg $l^{-1}$ for $Cl^-$ and $SO_4^{2-}$ (which required dilution). Precision errors were between 0.9 % ($SO_4^{2-}$) and 1.6 % ($PO_4^{3-}$), whilst the detection limit (three times the standard deviation of ten blanks) was $\leq$ 0.05 mg $l^{-1}$. Alkalinity was deduced by headspace analysis of an acidified (pH 1.7) sample of 10 ml immediately after return to the laboratory using a PP Systems EGM 4 infra-red gas analyser (precision errors 4.5%). Immediately in the field, the spring water outflow was analysed using Hach HQ40D meters for electrical conductivity and pH by gel electrode. To prevent the electrodes from freezing, this water was also injected by syringe into a pre-heated flow cell which maintained the water at about 7 °C.EC values in µS $cm^{-1}$ were transformed into general ion content values given as mg $l^{-1}$ by multiplication on 0.65.

## 4 Results

### 4.1 Ground temperature

The ground temperatures in borehole #9 on 12 September 2018 are shown in Fig. 2. At the lowermost sensor at 14.25 m bs the ground temperature reached –2.5 °C and varied at the same depth between –2.5 and –2.37 °C in the period from 15 May to 12

September 2018. The 0 °C point was observed at 1.5 m bs at the upper border of the massive pingo ice showing that the active-layer maximum depth reached the massive ice on 12 September 2018.

### 4.2 Cryolithology

#### 4.2.1 Core #9

The 25 m long core #9 drilled from the pingo top crater exposed cover and basal sedimentary horizons enclosing massive pingo ice (Fig. S1). From 0 to 1.5 m bs gravelly loam was found, which is assumed origin from the pingo top and moved downslope by cryoturbation and solifluction. Below this redeposited cover layer from 1.5 to 12 m bs transparent massive ice without any inclusions is observed. Air bubble content reaches up to 10 V% in single ice layers. In this particular layer and in all other layers of pingo massive ice bubbles are spherical and ~~chaotic~~irregularely distributed. Most common are bubbles with diameters near 1 mm but some bubbles rea~~i~~ch diameters up to 5 mm. Between 12 and 22.2 m bs the pingo ice remains transparent, but contains layers with 1-2 to 10-20 mm long large dark silty flakes in subvertical orientation (up to 0.5 V%). Alternating layers include rounded air bubbles (up to 10 V%). The total thickness of the massive pingo ice amounts to 20.7 m. Its lower contact to the basal deposits is well defined in the core. Massive pingo ice near the contact was not rich in air bubbles and had small admixture of previously mentioned dark silty flakes. The lowermost part ~~end~~ of the massive pingo ice in ~~our~~ core #9 was found at depth of 22.2 m bs. Below down to a depth of 25 m bs dark clay with regular reticulate and irregular reticulate cryostructures (ice lenses 2 to 20 mm thick) was found in the core. ~~From 22.2 to 25 m bs the massive pingo ice is underlain by dark grey clay with regular reticulate and irregular reticulate cryostructures (ice lenses 2 to 20 mm thick).~~At 23.8-24.3 m bs ice lenses were absent but 2-4 mm long lenses of black clay material were present. At 22.3-23.5 m bs and at 23.7-23.8 m bs layers of ~~clear (segregation) ice are found.~~transparent ice without inclusions and without air bubbles were found.

#### 4.2.2 Core #10

The core #10 drilled on top of the crater rim~~pingo~~ down to 12 m bs exposes sedimentary horizons (Fig. S1). The uppermost part from 0 to 2.5 m bs includes the modern top soil at 0 to 0.1 m bswith living shrub material and a buried soil formation at 0.25 to 0.4 m bs with decomposed similar shrub material.~~both notable by higher contents of plant organic material.~~ The minerogenic material is present by fine sand and loam including gravel. The cryostructures are wavy lenticular with ice lenses up to 2 cm thick. Toward 2.5 m bs the clay content increases as the gravel content decreases. ~~From 2.5 to 12 m bs, the clay shows subhorizontal lenticular cryostructures up to 2 cm thick and includes in ice oversaturated deposits and clear (segregation) ice at 4.7- 5.9 m bs, at 6.65-7.05 m bs and at 8.2-8.6 m bs although the massive ice of the pingo was not reached~~ From 2.5 to 12 m bs, the clay shows subhorizontal lenticular cryostructures up to 2 cm thick and includes ice-oversaturated deposits and ice with admixture of clay at 4.7- 5.9 m bs, at 6.65-7.05 m bs and at 8.2-8.6 m bs although the massive ice of the pingo was not reached. This ice and ice oversaturated deposits contain also sporadic gravel particles. In the layer 8.2-8.6 m ice

contained up to 10 V% of spherical air bubbles with diameter near to 1 mm. At 5.9 to 6.2 m bs a layer of sand and gravel (up to 3 cm in diameter) with organic remains is observed.

#### 4.2.3 Core #11

The core #11 was drilled in the surroundings of the pingo and reached a depth of 6 m bs, and is composed of gravelly sand and loam with structureless ~~cryostructure~~cryostructures (Fig. S1).

### 4.3 Isotopic and hydrochemical properties of the massive pingo ice and spring water

According to trends in stable water isotopic composition of the massive ice obtained in core #9, four units are distinguished, which are unit I to unit IV (Fig. 2; Table 1).

Unit I (1.1-9.8 m bs) shows a down-core decreasing trend in $\delta^{18}O$ and $\delta D$ from –9.6 to –16.8 ‰ and from –68 to –117 ‰, respectively, while the *d* increases from 8 to 18 ‰. Small inversions are notable at depths of 3.5 and 6.5 m bs (Fig. 2). The freezing of unit I is clearly expressed by $\delta^{18}O$-$\delta D$ and $\delta D$-*d* slopes of 6.7 and –0.2, respectively (Fig. 3). The ion composition of unit I is dominated by $Na^+$ and $K^+$ in cations and $Cl^-$ and $HCO_3^-$ in anions. Variations in total ion content (mean 22 mg $l^{-1}$) are triggered by variations in $Na^+$ (0-24 mg $l^{-1}$), $Cl^-$ (1-14 mg $l^{-1}$) and $HCO_3^-$ (1-40 mg $l^{-1}$) concentrations (Fig. 2, Table 2) while $NO_3^-$ and $SO_4^{2-}$ contents vary little around 1 mg $l^{-1}$ each. $Ca^{2+}$ occurs solely in the lowermost part of unit I with low concentration. The pH varies between 6.6 and 7.9.

The isotopic composition of the pingo ice in unit II (9.8-16.1 m bs) exhibits down-core the opposite pattern as in unit I with increasing trend in $\delta^{18}O$ and $\delta D$ from –16.7 to –11.1 ‰ and from –116 to –79 ‰, respectively, while the *d* decreases from 17 to 10 ‰ reaching almost the isotopic composition of the upper part of unit I (Fig. 2). The $\delta^{18}O$-$\delta D$ slope of 6.6 is slightly lower as in unit I while the $\delta D$-*d* slope of –0.2 is very close to that of unit I (Fig. 3). The pH increases down-core from 7 to 8.8 as the ion content does from 14 to 138 mg $l^{-1}$ (mean 72 mg $l^{-1}$, Table 2). The latter correlates to increasing concentrations of $Na^+$, $Cl^-$, $SO_4^{2-}$ and $HCO_3^-$, while $NO_3^-$ remains almost stable and $K^+$ decreases (Fig. 2).

The stable isotope composition of unit III (16.1-20.8 m bs) resembles those of unit I with down-core decreasing $\delta^{18}O$ and $\delta D$ from –10.8 to –15.2 ‰ and from –77 to –106 ‰, respectively. The *d* increases from 9 to 15 ‰. An inversion occurs at depth of 19.9 m bs (Fig. 2). The $\delta^{18}O$-$\delta D$ and $\delta D$-*d* slopes are almost the same as in unit II with values of 6.6 and –0.2, respectively (Fig. 3). The ion content reaches highest values up to 428 mg $l^{-1}$ (mean of 202 mg $l^{-1}$, Table 2) in the lower part of unit III due to increased $Na^+$, $Cl^-$ and $HCO_3^-$ concentrations, where also Mg occurs (Fig. 2). The pH varies between 7.8 and 8.9.

The lowermost unit IV (20.8-22.2 m bs) shows down-core increase in $\delta^{18}O$ and $\delta D$ and decrease *d* (Fig. 2) as unit II. The slopes of $\delta^{18}O$-$\delta D$ (–7.26) and $\delta D$-*d* (–0.23) are the lowest all pingo ice units (Fig. 3). The mean ion content of 53 mg $l^{-1}$is low (Table 2) due to largely reduced $Na^+$, $K^+$, $HCO_3^-$ and $Cl^-$ concentration (Fig. 2). The mean pH amounts to 7.8.

The overall pattern of the down-core isotopic composition of the pingo ice differentiates into to two modes of decreasing $\delta^{18}O$ and $\delta D$ and increasing *d* in units I and III and the opposite trends in units II and IV. The contents of $Na^+$, $Cl^-$ and $HCO_3^-$ ions

increase from unit I to III, while $K^+$ decreases from unit I to II and increases again in unit III, $NO_3^-$ and $SO_4^{2-}$ show rather low variation, and $Mg^{2+}$ and $Ca^{2+}$ occur only occasionally with concentrations above 0.25 mg $l^{-1}$.

The spring water sampled in the vicinity of the Oin pingo in 2018 is characterized by $\delta^{18}O$ of –13.01 ‰, $\delta D$ of –93.5 ‰ and *d* of 10.6 ‰ (Table 1). The ion content amounts to 1192 mg$l^{-1}$, with predominance of $HCO_3^-$ in anions (as indicated by the high alkalinity 2.2 mM $l^{-1}$), while $Cl^-$ and $SO_4^{2-}$ are found in concentrations of 15.3 and 3.8 mg$l^{-1}$respectively. The pH in the spring amounts to 8.8 (Table 2).

### 4.4 Hydrochemical properties of sedimentary water extracts

#### 4.4.1 Core #9

The hydrochemical signature of deposits underlying the massive ice of the pingo at 22.2 to 25 m bs is notable for high ion content reaching up to 1335 mg $l^{-1}$ and the prevalence of $Na^+$ and $HCO_3^-$ ions. (Fig. 4a, Table 3). Distinct ion content variations are driven by $Na^+$ and $K^+$ cations and $HCO_3^{2-}$ and $Cl^-$ anions. $Ca^{2+}$ and $Mg^{2+}$ have not been found and the anion composition resembles those of unit III. The pH is alkaline and varies between 9.2 and 9.9.

#### 4.4.2 Core #10

Core #10 drilled at the uppermost position of the pingo shows a different hydrochemical composition compared to the sedimentary water extracts than the bottom sediments of core #9 drilled nearby. The ion content is about nine times lower with mean values of about 99.6 mg $l^{-1}$ in core #10 and of about 1335 mg $l^{-1}$ in core #9 (Fig. 4a, b). The composition of major ions is also different with predominant $SO_4^{2-}$ and $HCO_3^-$ for anions while prevalent cations are still $Na^+$ and $K^+$. It is notable that $Ca^{2+}$ and $Mg^{2+}$ reach mean values of about 22 mg $l^{-1}$ and 2 mg $l^{-1}$, respectively (Table 3)~~), pointing to the non-marine origin of the deposits~~. The mean pH is neutral with 7.3±0.5.

#### 4.4.3 Core #11

The hydrochemical composition of major ions in core #11 generally resembles those of core #10 (Fig. 4b, c) although the ion content is much lower with a mean value of 38 mg $l^{-1}$ driven by more than two times lower $SO^4_{2-}$, ten times lower $Cl^-$, six times lower $Na^+$ and seven times lower $Ca^{2+}$ (Table 3). The pH is similar to those of core #10 with mean 7.2±0.3.

## 5 Discussion

### 5.1 Water sources of the massive pingo ice in Grøndalen

Following the current hypotheses on pingo growth on Spitsbergen, there are three possible main water sources for pingo massive ice formation, which are deep sub-permafrost groundwater for group I pingos connected to geologic fault structures,

sub-permafrost groundwater fed by sub-glacial melt for group II pingos and marine-originated groundwater for group III pingos (Matsuoka et al. 2004). Marine sources are assumed for hydraulic connections between groundwater of uplifted valleys after deglaciation and the sea (Yoshikawa and Harada, 1995). Sea ice, which is a result of seawater freezing is known to be sodium-chloride-dominated and shows ion contents between 2000 and 20000 mg $l^{-1}$ (Shokr and Sinha, 1995; Nazintsev and Panov, 2000) depending on freezing velocity, temperature and age. The massive ice of the pingo in Grøndalen shows prevalent $Na^{+}$-$HCO_3^{-}$ contents and ion content with maximum values of 428 mg $l^{-1}$ (mean of 78±101mg $l^{-1}$, Table 2). Thus, marine sources for the pingo massive ice are excluded and the previous assignment of the Grøndalen pingos to ancient group III pingos by Yoshikawa and Harada (1995) seems unlikely. Precipitation and surface waters in Grøndalen have lower ion contents and different composition if compared to the pingo massive ice (Table 2), which also excludes these sources as the main ones for the pingos of Grøndalen. The role of artesian flow resulting from the migration of sub-glacial groundwater for pingo formation on Spitsbergen has been previously studied by Liestøl (1977, 1996) and Yoshikawa and Harada (1995). The original hydrochemical signature of water released from glacial melt is certainly altered by subsurface migration through various deposits. Pressurised spring water from beneath an ice blister sampled in 2018 shows predominance of $HCO_3^{-}$ in anions and ion content of 1192 mg$l^{-1}$ (Table 2). Furthermore, in 1921 the Norwegian geologist Anders K. Orvin described a spring in Grøndalen and sampled spring water in 1926 (Orvin, 1944), approximately at the northern side of today's Gloin pingo (Fig. 1). This data from spring found in 2018 and 1926 seem meaningful to explore the potential water source for the pingo formations. The spring water analysed by Orvin was characterised by prevalent $Na^{+}$ and $HCO_3^{-}$ ions, which is typical for freshwater hydrogeological structures below permafrost (Romanovskiy, 1983), and an ion content of 879 mg $l^{-1}$ (Table 2). The sedimentary water-extract data from deposits underlying the massive ice shows likewise prevalent $Na^{+}$ and $HCO_3^{-}$ ions (Table 3). The similarity of the ion compositions of the spring water and the water extract of deposits underlying the massive ice to those of the Fili pingo ice is striking although the absolute concentrations are much higher in the spring (1192 mg $l^{-1}$ in 2018 and 879.2 mg $l^{-1}$ in 1926) than in the massive ice (mean of all core#9 units 79.0±102.4).This difference between the ion concentrations in the spring water and in the pingo ice is most likely explained by salt expulsion during freezing, which is typical for ice formation from fresh groundwater (Romanovskiy, 1983). We therefore conclude that the groundwater feeding the springs observed by Orvin (1944) and later within this study represents the main source water for the massive pingo ice. This interpretation is further supported by the chain-like distribution of spring and pingos from east to west across the Grøndalen (Fig. 1b), which might delineate connectivity for sub-permafrost groundwater by the fault zone further protruding towards the Bøhmdalen.

It was suggested that groundwater recharge in Spitsbergen is related to the warm-based glaciers as there are no other potential taliks where groundwater recharge can occur (Orvin, 1944; Liestøl, 1976). Glaciers on the mounts surrounding the valley ~~on the mounts of valley sides~~ occur just several kilometres to the north from the Grøndalen pingos (Fig. 1), namely Irabreen and Stolleybreen. The water temperature is close to 0 °C when it is recharged below the glacier. Taking into account geothermal gradient of ~2 °C per 100 m in the coal survey wells in Barentsburg closest to the studied pingo (Ershov, 1998) and the fact that the base of surrounding glaciers is approximately at 500 m asl and pingos and spring are located between 100 and 50 m

asl, geothermal heat will increase water temperature melted on the glacier base during its transit through the aquifer to the spring location directly to 9 °C as was observed by Orvin in 1921 (Orvin, 1944). Together with low salt content of the spring water, this observation allow suggesting that the source of sub-permafrost water discharged by the spring (and responsible for pingo formation) was sub-glacial melt heated and slightly salted during its rather fast transport through the aquifer to the discharge area.

### 5.2 Stable water isotope composition of the pingo massive ice in Grøndalen

Assuming a conical geometry of the pingo ice body that grew equally to all sides, the chosen central drilling position on top of the pingo and the strictly vertical drilling allowed capturing freezing stages of the massive ice. Variations in the isotopic composition of the four massive pingo-ice units and between them might be explained by three main controls. Firstly, isotopic variations in the pingo ice might correspond to differing water sources migrating towards the freezing front during different periods of ice formation. Secondly, the source water of the pingo ice was constant, but had distinctly differing isotopic signatures over time. And thirdly, the isotopic variations of the pingo ice represent changes in closed, (semi-closed) and open system condition, i.e. freezing of a fixed or a (partly) renewed water volume. ~~Estimations of pingo growth rate in Siberia and North America shows values of order decimetres per year (Chizhova and Vasil'chuk, 2018). That is why, concerning the first and the second controls, we assume rather no or only little changes in the water source and its isotopic composition over the rather small period of pingo formation.~~ Estimations of pingo growth rate in Siberia and North America may reach values of order decimetres per year (Mackay, 1979; Chizhova and Vasil'chuk, 2018). Assuming a similar fast growth of the Fili pingo no or only little changes in isotopic composition of water source over the rather short period of pingo formation are likely. Thus, we assume the second controls on isotopic composition of the Fili pingo massive ice of less importance. The isotopic composition of spring water sampled in Grøndalen in 2018 shows –13.01 ‰ in $\delta^{18}O$, –93.5 ‰ in δD and a *d* of 10.6 ‰, which is very close to the respective mean values of the massive pingo ice (all units) of –12.56±2.14‰ in $\delta^{18}O$, –89.0±14.2‰ in δD and a *d* of 11.5±4.1‰ (Table 1, Figure 3b, c). This observation makes it likely that the sub-permafrost groundwater feeding the spring also maintained the massive pingo-ice formation. Thus, the most probable explanation for the observed isotopic composition of the massive pingo ice relates to subsurface hydrologic conditions, i.e. the system state of closed or open conditions, which are further controlled by local groundwater pressure and the position of the permafrost table. Concurrent changes in the system character from closed to open as deduced from the isotopic and chemical compositions of the pingo ice units are outlined and discussed below.

The isotopic stratification of the massive pingo ice differentiates into four stages of pingo growth. The earliest stage of massive ice formation is represented in unit I (1.5-9.8 m bs). The down-core strong decline within unit I by about 7‰ $\delta^{18}O$, 49 ‰ in δD accompanied by a strong rise of 10 ‰ in *d* (Fig. 2) indicates a high near-surface temperature gradient, fast freezing and fast formation the about 8-m-thick unit I. If compared to a closed-system freezing model of Ekaykin et al. (2016), the down-core isotopic depletion in unit I is close to the modelled one (Fig. 5a) if an initial isotopic composition of –12.6 ‰ in $\delta^{18}O$ and –88 ‰ in δD is assumed. This is much lower than the modern mean annual precipitation values in the Barentsburg region with

–9.0±4.2 ‰ in $\delta^{18}O$ and –64±30 ‰ in δD, and closer to mean values of the Grøn River and its tributaries with about –11.7±0.3 ‰ in $\delta^{18}O$ and –78±3 ‰ in δD (Table 1). Thus, if precipitation was the main source of the massive ice, its onset took place during a colder period than today. More likely, the underground water sources feeding spring near the pingo was the same source for the ~~the Grøn River system, which are glacial meltwater and subsurface discharge represent the main water source of the~~ massive pingo ice. According to the model, the lowermost (last formed) ice of unit I at a depth of 9.6 m bs corresponds to 85 % frozen water of the initial volume. If so the remaining unfrozen water would have had a highly depleted composition of about –19.0 ‰ in $\delta^{18}O$ and –130 ‰ in δD (Fig. 5b). However, the modelled data do not entirely catch the real distribution of unit I isotopic composition where the $\delta^{18}O$ values are slightly below and the *d* values slightly above the respective modelled lines (Fig. 5b). Because the model uses the maximum fractionation coefficient (Souchez and Jouzel, 1984), higher fractionation during freezing than modelled is impossible. Therefore, the system during freezing of unit I was likely not completely closed and new source water entered the system when about 50 % of the water was already frozen and changed the isotopic composition of the remaining unfrozen water. This is supported by the slight reversal in $\delta^{18}O$ and δD, a more distinct reversal in *d*, and higher ion concentrations at depth of 6.5 m bs (Fig. 2). In Fig. 5a is shown that the last six most depleted $\delta^{18}O$ data points after about 50% of the water are frozen (corresponding to the lowermost data points of unit I in Fig. 2) increasingly deviate from the modelled data. Freezing of large parts of the unit I massive ice at least in only two stages under closed-system conditions is deduced.

The massive ice of unit II (9.8-16.1 m bs) is characterised by down-core increasing $\delta^{18}O$ and δD by about 5.6 ‰ and 37 ‰, respectively. The *d* decreases by about 8 ‰ (Fig. 2). Such down-core pattern might be explained by freezing under semi closed-system conditions when the water reservoir got episodically renewed with isotopically less depleted subsurface water. The observed down-core increase in solute concentrations of the unit II ice (Fig. 2) further indicates ion enrichment in the source water during ongoing freezing, and therefore questions the occurrence of a completely open system fed by constant water supply.

The down-core isotopic composition of unit III (16.1-20.8 m bs) resembles those of unit I with declining $\delta^{18}O$ by about 4.4 ‰ and δD by about 29 ‰ concurrent with a rising *d* by about 6 ‰ (Fig. 2). Reversals in $\delta^{18}O$ and δD and corresponding *d* are observed at depth of 19.9 m bs (Fig. 2), pointing to similar changes of the recharge reservoir as described for unit I. If compared to the freezing model under closed-system conditions (Fig. 5c) the water forming the ice of unit III would have had an initial composition of –14.4 ‰ in $\delta^{18}O$ and –101 ‰ in δD. The more depleted isotopic values if compared to unit I are likely explained by fractionation of the available water volume due to previous freezing and formation of the older massive ice units. The lowermost ice of unit II (–11.1 ‰ $\delta^{18}O$, –79 ‰ δD) is isotopically very close to the uppermost ice of unit III (– 10.8 ‰ $\delta^{18}O$, –77 ‰ δD), pointing to freezing of the same source water. The lowermost (last formed) ice of unit III at a depth of 20.5 m bs represents about 75 % frozen water of the initial reservoir (Fig. 5d) and points as the record of unit I again to freezing of a substantial part of the massive pingo ice (4.7 m thickness) of under prevailing closed-system conditions. The down-core increase in solute concentrations with highest values in the lowermost part of unit III supports closed-system freezing conditions of a fixed water volume.

The lowermost unit IV (20.8-22.2 m bs) exhibits down-core increasing $\delta^{18}O$ by about 2 ‰ and δD by about 15 ‰ while *d* decreases by about 3 ‰similarly to unit II but at less ranges. A drop in solute concentrations is striking (Fig. 2). Both, hydrochemical and isotopic composition of unit IV point to freezing conditions of a semi-closed system.

In summary, the pingo ice record obtained in core #9 delineates two closed-system freezing episodes (units I and III) with only slight recharge inversions of the water reservoir and two episodes (units II and IV) with more complicated freezing of subsurface water under semi-closed conditions when the reservoir got renewed from the same source. ~~A changing water source from less glacial runoff to more precipitation driven water sources might also induce the observed down core increase in $\delta^{18}O$ and δD and the accompanying decrease in *d*. Generally increasing $\delta^{18}O$ and δD values are not associated with changes in the freezing that produces constant to decreasing values from open to closed system.~~

Nowadays, the pingo has already accomplished its active growth as seen by the degradation crater on top of the pingo and the occurrence frozen deposits underlying the massive pingo ice. The latter induces that the freezing front where the pingo ice formed disappeared when the ground got deeply frozen. The relatively warm ground temperature of only –2.5 °C at 14.25 m bs in borehole #9 and the active layer reaching the top of the massive ice lead to its successive melt and intensified solifluction further lowering the thickness of the protective layer above the massive ice. As a further consequence of ongoing degradation of the pingo, the crater lake (20 x 30 m) might develop into a larger thermokarst lake as the massive ice melt proceeds. Such solifluction and thermokarst degradation processes are common for Spitsbergen pingos (Liestøl, 1996).

### 5.3 Some aspects of pingo formation in the context of Grøndalen valley history

The elongated outer shape of the Fili pingo cone is also observed for other pingos on Spitsbergen (Liestøl, 1996) while the revealed information on the internal structure of Fili pingo is unique in the sense that it is the only pingo completely drilled in its centre. The Riverbed pingo in Adventdalen as referred in (Matsuoka et al., 2004) unfortunately was studied for other purposes, and it exposure in a distal position doesn't allow to comparison with the Fili pingo in Grøndalen, where borehole in the centre of mound ~~The observations of the Riverbed pingo in Adventdalen where river erosion removed the slope deposits and exposed ice, gravel and sand in a distal position of the pingo (Matsuoka et al., 2004) are, however, not directly comparable in exposure and internal structure to those of Fili pingo that~~ exhibits the entire massive ice ~~in its central position~~.

The shape of the massive pingo ice can be deduced in vertical extension from its upper and lower boundaries observed in core #9 between 1.5 and 22.2 m bs. In lateral extension, the core #10 drilled from the crater top down to 12 m bs in about 35 m distance from the core #9 position did not reach the massive ice and suggests a rather steep slope of the massive ice body. The assumed shape of the pingo and its massive ice is shown in Fig. 1c. The thickness of the massive ice (20.7 m) exceeds the height of the pingo of 9.5 m, which is explained by ~~step wise~~ massive ice growth when the ongoing subsurface freezing pushed the previously formed ice and cover deposits upward. The latter moved subsequently from the pingo top down-slope by solifluction. Thus, the 9.5 m amplitude of surface uplift seen in the modern stage of pingo evolution became less than the 20.7 m thickness of the massive ice. Solifluction further explains the presence of the buried soil observed at 0.25-0.4 m bs in core #10. If these assumptions are reliable, the massive ice formation started at the freezing front at a depth of about 15 m bs.

Because the ongoing freezing of new ice below the previously formed massive ice is only possible at the contact between ice and unfrozen waterlogged deposits, it seems likely that the advance of the freezing front got compensated by the growth of the massive ice and the pingo heave as well as by geothermal heat transported by groundwater. Consequently, the ground temperature at the base of the massive ice remained at the freezing point during the pingo growth. Even if the advance of the freezing front slowed somewhat down by massive ice formation, pingo growth and geothermal heat from groundwater, the latter did not slow down the freezing of the cover deposits along the shape of the aggrading hill, which likely promoted lateral freezing from the slopes, and terminated pingo growth.

Because information on the origin and ages of the deposits surrounding the pingos of Grøndalen are still lacking, such aspects will be addressed in future work. Nevertheless, tentative assumptions of the pingo formation stages in context of the valley evolution can already be~~en~~ drawn. ~~While pingo formation in general depends on freezing of loose deposits and water migration towards the freezing front, the presence of pingos in Grøndalen confirm epigenetic freezing of formerly unfrozen deposits.~~Yoshikawa and Harada (1995) conclude from the position of the Grøndalen pingos at about 50 m asl that their formation started quickly after retreat of the sea (Fig. 6).

After retreat of the sea and establishment of the Grøn River system, we assume a sedimentation period of non-marine gravelly sand and loam deposits observed in core #11. These deposits also covers the top and the slopes of the Fili pingo (core #10) and represent therefore the non-marine ground in which the Grøndalen pingos formed, contradicting the interpretation of Yoshikawa and Harada (1995) who proposed pingo growth within refreezing marine sediments after sea regression. Based on the finding of lower ice body boundary at the depth 15 m under the surrounding surface (Fig. 1c), the position of the freezing front is assumed to have reached this depth before start of pingo growth. To reach such depth, we further assume a certain period of time that was also needed to disconnect the groundwater hydrology of the valley from the sea since seawater is unlikely to have been the source of the pingo massive ice as discussed above. The aggrading permafrost in Grøndalen likely restructured the groundwater hydrogeology of the valley and created groundwater flow in the fault zone connected to Bøhmdalen and Grøndalen that fed the ~~Grøndalen~~pingos and explains their chain-like occurrence (Fig. 1b). Comparable to the pingo formation in Adventdalen, where the oldest pingos developed at higher positions (Fig. 6b), more distant from the sea (Yoshikawa and Nakamura, 1996)~~, we propose a similar pattern in Grøndalen.~~ If this assumption is correct for Grøndalen, Nori pingo is the youngest and Gloin pingo is the oldest in the pingo chain of Grøndalen (Fig. 1b). While the taliks feeding the oldest pingos (above 50 m asl) froze subsequently, the next connectivity at lower topography became the place for new pingo formation and thus creating a chain of pingos following fault zone and the downslope topographic gradient and hence the availability of groundwater (Fig. 6c). The activity of groundwater springs related to warm-based glaciers might reflect their shrinking by less discharge of even disappearance of the springs (Haldersen et al., 2011). This is because glacier size decrease and surface lowering induce shrinking accumulation area and further decreasing warm-based area terminating the recharge of springs. In this context, in the study of Chernov and Muraviev (2018) it was shown that the loss in glacier area in Nordenskiöld Land (West Spitsbergen) between 1936 and 2017 reached 49.5 %. Water discharge by the spring in Grøndalen does not necessarily means that surrounding glaciers are warm-based at current time. They are probably cold-based today because of

their current small size, but meltwater from the stage when they were warm-based may still be discharged by Grøndalen springs due to low discharge rates ~~at rare locations~~. Pingos in Grøndalen accomplished their growth not because of stop of ground water flow but because of freezing of sediments below the massive ice inhabiting the water supply. Today Grøndalen pingos exhibit clear degradation features such as the crater lake on top of Fili pingo (Fig. 6d).

## 6 Conclusions

For the first time a pingo on Spitsbergen was completely drilled to obtain records of the massive ice and the deposits above and the permafrost below it. The massive pingo ice is almost clear and reaches a thickness of 20.7 m while the pingo reaches a height above the surrounding surface of 9.5 m at present. Both, pingo ice thickness and pingo height were reduced by degradation. The lowermost measured ground temperature at 14.25 m bs close to the zero-amplitude temperature showed only little variation between –2.5 and –2.37 °C from May to September 2018. The ~~active layer depth~~maximum thaw depth of 1.5 m in September 2018 reached the uppermost massive ice, which indicates the ongoing fast degradation of the pingo. This is further seen in the crater lake on top of the pingo and strong solifluction that removes cover deposits downslope.

The stable water isotope record of the massive ice shows two episodes of closed-system freezing and two episodes of semi-closed freezing when the source water feeding the massive ice formation recharged. The hydrochemical composition of the massive ice and the permafrost below is dominated by $Na^+$ and $HCO_3^-$ ions, thus of terrestrial origin and similar to those of historical and modern observations of springwater in Grøndalen.

Our current understanding of pingo-related processes and conditions in Grøndalen makes it difficult to align them to the pingo categories for Spitsbergen proposed by Yoshikawa and Harada (1995). ~~We identified characteristics such as fault-related groundwater discharge (aligned to group I) and ground-water origin from warm-based glaciers (aligned to group II) while their formation within epigenetically refreezing marine deposits immediately after sea regression (aligned to group III) seem unlikely due to the non-marine character of the deposits surrounding the Grøndalen pingos.~~In the Fili pingo record of Grøndalen we concurrently identified pingo-formation characteristics such as fault-related groundwater discharge (typical for group I pingos) and ground-water origin from warm-based glaciers (typical for group II pingos). The proposed pingo formation in Grøndalen is connected to epigenetic refreezing of marine deposits (typical for group III pingos) but not immediately after sea regression due to the reworking of marine sediments seen in deposits surrounding the Grøndalen pingos.

~~Pingos are highly sensitive to climate warming, there origin and distribution over Spitsbergen valleys depends on complex interaction of hydrogeological structures with climate, sea, glaciers, permafrost and, thus their further investigation is one of the keys to understanding history of climate evolution.~~The origin and distribution of pingos in Grøndalen depends on the complex interaction of hydrogeological conditions and sea level, glaciers and permafrost dynamics superimposed by climate variability over time. The latter may be typical for vast archipelago and makes investigation of pingos important for understanding key stages of cryosphere evolution of Spitsbergen.

## Author contributions

ND and SV initiated and designed the present study. They further drilled and documented the cores together with VD. AE carried out stable isotope analyses. AE and AJH contributed hydrochemical and stable isotope data of the modern environment, such as from precipitation, surface waters and sources. MA, LS and HM supported the overall data analysis and interpretation. ND and SW wrote the paper with input from the other co-authors, who contributed equally to the final discussion of the results and interpretations.

## Competing interests

The authors declare that they have no conflict of interest.


## Acknowledgements

This work is supported by the Russian Science Foundation (grant № 19-77-10066). We acknowledge support for field logistics and lab analytics from the Russian Scientific Arctic Expedition on Spitsbergen Archipelago (RAE-S), Barentsburg. Ekaterina Poliakova (Arctic and Antarctic Research Institute, St. Petersburg, Russia) provided useful translations of Norwegian original literature. SW was supported by Deutsche Forschungsgemeinschaft (grant no. WE4390/7-1). AH acknowledges JPI-Climate Topic 2: Russian Arctic and Boreal Systems, Award No. 71126 (LowPerm). We thank our referees Trevor Porter and Go Iwahana as well as the handling editor Peter Morse for critical and helpful comments to improve the final version of the paper.


## References


Burr, D.M., Tanaka, K.L., and Yoshikawa, K.: Pingos on Earth and Mars, Planetary and Space Science, 57(5-6), 541-555, https://doi.org/10.1016/j.pss.2008.11.003, 2009.

Chernov, R.A., and Muraviev, A.Ya.: Contemporary changes in the area of glaciers in the western part of the Nordenskjold Land (Svalbard), Ice and Snow (Лёд и Снег), 58(4), 462-472, doi: 10.15356/2076-6734-2018-4-462-472, 2018 (in Russian).

Chizhova Ju.N., and Vasil'chuk Yu.K.: Use of stable water isotopes to identify stages of the pingo ice core formation, Ice and Snow (Лёд и Снег), 58 (4), 507–523, doi: 10.15356/2076-6734-2018-4-507-52, 2018 (in Russian).

Christiansen, H.H., Gilbert, G.L., Demidov, N., Guglielmin, M., Isaksen, K., Osuch, M., and Boike, J.: Permafrost thermal snapshot and active-layer thickness in Svalbard 2016-2017, In: SESS report 2018, The State of Environmental Science in Svalbard – an annual report, Eds.: Orr, E., Hansen, G., Lappalainen, H., Hübner, C., Lihavainen, H., SIOS, Longyearbyen, Svalbard, pp. 26-47, https://www.sios-svalbard.org/sites/sios-svalbard.org/files/common/SESSreport_2018_FullReport.pdf, 2019.

Dansgaard, W.: Stable isotopes in precipitation, Tellus, 16(4), 436-468, https://doi.org/10.3402/tellusa.v16i4.8993, 1964.

Demidov, N.E., Verkulich, S.R, Karaevska, E.S., Nikulina, A.L., and Savatyugin, L.M.: First results of permafrost observations at the monitoring site of the Russian Scientific Centre on Spitsbergen (ПервыерезультатымерзлотныхнаблюденийнакриосферномполигонеРоссискогонаучногоцентранаархипелагеШпицберген (РНЦШ)), Problems of the Arctic and Antarctic (Проблемы Арктики и Антарктики), 2016 № 4(110), 67-79, 2016 (in Russian).

Ekaykin, A.A., Lipenkov, V.Ya.,Kozachek, A.V., and Vladimirova, D.O.: Stable water isotopic composition of the Antarctic subglacial Lake Vostok: implications for understanding the lake's hydrology, Isotopes in Environmental and Health Studies, 52 (4-5), 468-476, http://dx.doi.org/10.1080/10256016.2015.1129327, 2016.

French, H., and Shur, Y.: The principles of cryostratigraphy, Earth-Science Reviews, 101, https://doi.org/10.1016/j.earscirev.2010.04.002, 190-206, 2010.

Geological map Svalbard 1:100 000, Spitsbergen Norsk Polarinstitutt Temakart nr. 16, 1991

Ershov, E.D. (Ed.): Fundamentals of Geocryology. Volume III. Regional and historical geocryology of the world (Основыгеокриологии. Ч. 3. Региональная и историческаягеокриологияМира). Moscow University Publishing House, Moscow, 575 pp., 1998 (in Russian).

Grosse, G., and Jones, B.M.: Spatial distribution of pingos in northern Asia. Cryosphere, 5, 13-33, https://doi.org/10.5194/tc-5-13-2011, 2011.

Haldorsen S., Heim M., and van der Ploeg M. J.: Impacts of climate change on groundwater in permafrost areas: case study from Svalbard, Norway. In: Climate change effects on groundwater resources: A global synthesis of findings and recommendations, Eds.: Treidel, H., Martin-Bordes, J.L., and Gurdak, J.J., CRC Press, Boca Raton, FL, USA, pp. 323-338, 2011.

Hjelle, A.: Geology of Svalbard, Polar håndbok No. 7, Norsk Polarinstitutt, Oslo, Norway, 1993.

Hyvärinen, H., and Ritchie, J.C.: Pollen stratigraphy of Mackenzie pingo sediments, N.W.T., Canada. Arctic and Alpine Research, 7, 261-272, doi:10.1080/00040851.1975.12003832, 1975.

Ishikawa, M., and Jambaljav, Ya.: Formation chronology of Arsain pingo, Darhad Basin, Northern Mongolia, Permafrost Periglacial Process., 27(3), 297-306, https://doi.org/10.1002/ppp.1877, 2016.

Jones, B.M., Grosse, G., Hinkel, K.M., Arp, C.D., Walker, S., Beck, R.A., and Galloway, J.P.: Assessment of pingo distribution and morphometry using an IfSAR derived DSM, western Arctic Coastal Plain, northern Alaska, Geomorphology, 138, 1-14, https://doi.org/10.1016/j.geomorph.2011.08.007, 2012.

Souchez, R., and Jouzel, J.: On the isotopic composition in δD and $\delta^{18}O$ of water and ice during freezing. J. Glaciol., 30(106), 369-372, https://doi.org/10.3189/S0022143000006249, 1984.

Liestøl, O.: Pingos, springs, and permafrost in Spitsbergen. Norsk Polarinstitutt Årbok 1975, 7-29, 1977.

Liestøl, O.: Open-system pingos in Spitsbergen. Norsk Geografisk Tidsskrift, 50(1), 81-84, https://doi.org/10.1080/00291959608552355, 1996.

Mackay, J.R.: Pingos of the Pleistocene Mackenzie Delta area, Geographical Bulletin, 18, 21-63, 1962.

Mackay, J.R.: Pingos of the Tuktoyaktuk Peninsula Area, Northwest Territories. Géographie physique et Quaternaire, 33 (1), 3-61, https://doi.org/10.7202/1000322ar, 1979.

Mackay, J.R.: Growth of Ibyuk Pingo, western Arctic coast, Canada, and some implications for environmental reconstructions, Quat. Res., 26(1), 68-80, https://doi.org/10.1016/0033-5894(86)90084-0, 1986.

Matsuoka N., Sawaguchi S., and Yoshikawa K.: Present-day periglacial environments in Central Spitsbergen, Svalbard, Geographical Review of Japan, 77(5), 276-300, https://doi.org/10.4157/grj.77.276, 2004

Nazintsev U.L., and Panov V.V.: Phase composition and thermophysical properties of sea ice (Фазовыйсостав и теплофизическиехарактеристикиморскогольда), Gidrometeoizdat, St. Petersburg, Russia, 83 pp., 2000 (in Russian).

Orvin A.K.: Litt om Kilder pa Svalbard, Norsk Geografisk Tidsskrift, X(1), 16-38, 1944 (in Norwegian).

Palagushkina, O., Biskaborn, B., Wetterich, S., Schirrmeister, L., Nazarova, L., and Grosse, G.: Modern and fossil freshwater diatoms (Bacillariophyceae) in periglacial environments of the Seward Peninsula (northwestern Alaska), Paleogeogr. Paleoclimatol. Paleoecol., 479, 1-15, https://doi.org/10.1016/j.palaeo.2017.04.006, 2017.

Romanovskiy, N.N.: Underground Waters of the Permafrost Zone (Подземные воды криолитозоны). Moscow State University Press, Moscow, Russia, 232 pp., 1983 (in Russian)

Ross, N., Harris, C., Christiansen, H.H., and Brabham, P.J.: Ground penetrating radar investigations of open system pingos, Adventdalen, Svalbard, Norsk Geografisk Tidsskrift, 59(2), 129-138, https://doi.org/10.1080/00291950510020600, 2005.

Rossi, G., Accaino, F., Boaga, J., Petronio, L., Romeo, R., and Wheeler, W.: Seismic survey on an open pingo system in Adventdalen Valley, Spitsbergen, Svalbard, Near Surface Geophysics, 16(1), 1-15, doi: 10.3997/1873-0604.2017037, 2018.

Shokr, M., and Sinha, N.: Sea ice: physics and remote sensing, John Wiley and Sons, Chichester, UK, 2015.

Skakun, A.A., Chikhachev, K.B., Ekaykin, A.A., Kozachek, A.V., Vladimirova, D.O., Veres, A.N., and Verkulich, S.R., Sidorova, O.R., and Demidov, N.E.: Stable isotopic content of atmospheric precipitation and natural waters in the vicinity of Barentsburg (Svalbard),Ice and Snow (Лёд и Снег), in review.

Tolkien, J.R.R.: The Lord of the Rings. Allen and Unwin, Norwich, UK, 1954-1955.

Ulrich, M., Wetterich, S., Rudaya, N., Frolova, L., Schmidt, J., Siegert, C., Fedorov, A.N., and Zielhofer, C.: Rapid thermokarst evolution during the mid-Holocene in Central Yakutia, Russia, Holocene, 27(12), 1899-1913, https://doi.org/10.1177/0959683617708454, 2017.

van Everdingen, R.E.: Multi-language glossary of permafrost and related ground-ice terms (revised 2005), Boulder, USA: National Snow and Ice Data Center/World Data Center for Glaciology, 1998.

Verkulich, S., Zazovskaya, E., Pushina, Z., Savelieva, L., Soloveva, D., Demidov, N., Shishkov, V., and Dercon, G.: The postglacial environmental changes in vicinity of the Barentsburg settlement (West Spitsbergen), EGU General Assembly, Vienna, Austria, 8-13 April 2018, EGU 2018-7729, 2018.

Wetterich, S., Grosse, G., Schirrmeister, L., Andreev, A.A., Bobrov, A.A., Kienast, F., Bigelow, N.H., and Edwards, M.E.: Late Quaternary environmental and landscape dynamics revealed by a pingo sequence on the northern Seward Peninsula, Alaska, Quat. Sci. Rev., 39, 26-44, https://doi.org/10.1016/j.quascirev.2012.01.027, 2012.

Wetterich, S., Schirrmeister, L., Nazarova, L., Palagushkina, O., Bobrov, A., Pogosyan, L., Savelieva, L., Syrykh, L., Matthes, H., Fritz, M., Günther, F., Opel, T., and Meyer, H.: Holocene thermokarst and pingo development in the Kolyma Lowland (NE Siberia). Permafrost Periglacial Process., 29(3), 182-198, https://doi.org/10.1002/ppp.1979, 2018.

Yoshikawa, K.: Notes on Open-System Pingo Ice, Adventdalen, Spitsbergen. Permafrost Periglacial Process., 4(4), 327-334, https://doi.org/10.1002/ppp.3430040405, 1993.

Yoshikawa, K., and Harada, K.: Observations on nearshore pingo growth, Adventdalen, Spitsbergen, Permafrost Periglacial Process., 6(4), 361-372, https://doi.org/10.1002/ppp.3430060407, 1995.

Yoshikawa, K., and Nakamura, T.: Pingo growth ages in the delta area, Adventdalen, Spitsbergen. Polar Record, 32(183): 347-352, https://doi.org/10.1017/S0032247400067565, 1996.

Yoshikawa, K., Leuschen, C., Ikeda, A., Harada, K., Gogineni, P., Hoekstra, P., Hinzman, L., Sawada, Y., andMatsuoka, N.: Comparison of geophysical investigations for detection of massive ground ice (pingo ice), J. Geophys. Res., 111, E06S19, doi:10.1029/2005JE002573, 2006.

Yoshikawa, K., Natsagdorj, S., and Sharkhuu, A.: Groundwater hydrology and stable isotope analysis of an open-system pingo in northwestern Mongolia. Permafrost Periglacial Process., 24(3), 175-183, https://doi.org/10.1002/ppp.1773, 2013.

## Tables

**Table 1: Stable isotope ($\delta^{18}O$, $\delta D$, and *d*) minimum, mean, maximum values, standard deviations (std), and slopes, intercept and correlation coefficient ($r^2$) of $\delta^{18}O$-$\delta D$ and $\delta D$-*d* plots from massive pingo ice of core #9, from intrasedimental ice of core #10 and from precipitation (2016-2018). Data are shown in Fig. 3. Additional data from 2018 include spring water of Grøndalen and river and tributary water of the Grøn River (Skakun et al., in review).**

| **Material** | | **core #9 unit I** | **core #9 unit II** | **core #9 unit III** | **core #9 unit IV** | **core #9 units I-IV** | **core #10** | **Modern precipitation** | **Grøn River and tributaries** | **Grøndalen spring** |
|---|---|---|---|---|---|---|---|---|---|---|
| Core depth | [m bs] | 1.5-9.8 | 9.8-16.1 | 16.1-20.8 | 20.8-22.2 | 1.4-22.2 | 6.65-8.4 | surface | surface | surface |
| n | | 16 | 10 | 7 | 3 | 38 | 4 | 88 | 7 | 1 |
| $\delta^{18}O$ min | [‰] | –16.81 | –16.65 | –15.18 | –12.80 | –16.81 | –18.93 | –18.42 | –11.71 | -- |
| $\delta^{18}O$ mean | [‰] | –12.56 | –13.06 | –13.17 | –11.42 | –12.56 | –14.09 | –8.95 | –11.24 | –13.01 |
| $\delta^{18}O$ max | [‰] | –9.56 | –11.07 | –10.80 | –10.60 | –9.52 | –11.98 | –0.80 | –10.89 | -- |
| $\delta^{18}O$ std | [‰] | 2.26 | 2.34 | 1.58 | 1.20 | 2.14 | 3.25 | 4.23 | 0.27 | -- |
| $\delta D$ min | [‰] | –116.9 | –115.9 | –106.3 | –90.7 | –116.9 | –131.3 | –144.5 | –83.2 | -- |
| $\delta D$ mean | [‰] | –88.9 | –92.0 | –93.1 | –81.7 | –89.0 | –98.8 | –64.2 | –78.1 | –93.5 |
| $\delta D$ max | [‰] | –68.4 | –78.8 | –77.2 | –6.1 | –68.4 | –84.4 | –17.3 | –75.2 | -- |
| $\delta D$std | [‰] | 15.1 | 15.4 | 10.5 | 7.9 | 14.2 | 21.9 | 30.2 | 2.6 | -- |
| *d* min | [‰] | 8.0 | 9.7 | 9.2 | 8.5 | 7.6 | 11.5 | –25.0 | 10.5 | -- |
| *d* mean | [‰] | 11.5 | 12.4 | 12.3 | 9.7 | 11.5 | 13.9 | 7.5 | 11.9 | 10.6 |
| *d* max | [‰] | 17.6 | 17.4 | 15.1 | 11.7 | 17.6 | 20.1 | 45.1 | 13.3 | -- |
| *d* std | [‰] | 3.1 | 3.3 | 2.2 | 1.8 | 2.9 | 4.1 | 10.8 | 1.3 | -- |
| Slope | $\delta^{18}O$-$\delta D$ | 6.66 | 6.60 | 6.58 | 6.52 | 6.63 | 6.74 | 6.78 | 8.18 | -- |
| Intercept | $\delta^{18}O$-$\delta D$ | -5.28 | –5.88 | –6.46 | –7.26 | –5.67 | -3.81 | –3.39 | +13.92 | -- |
| $r^2$ | $\delta^{18}O$-$\delta D$ | 1 | 1 | 1 | 1 | 1 | 1 | 0.90 | 0.75 | -- |
| Slope | $\delta D$-*d* | –0.20 | –0.21 | –0.21 | –0.23 | –0.21 | -- | -- | -- | -- |
| Intercept | $\delta D$-*d* | –6.26 | –7.10 | –7.72 | –8.78 | –6.77 | -- | -- | -- | -- |
| $r^2$ | $\delta D$-*d* | 0.97 | 0.99 | 0.96 | 0.97 | 0.98 | -- | -- | -- | -- |

**Table 2: Hydrochemical composition of the massive pingo ice of core #9 given as minimum, mean, maximum values, standard deviations (std) per unit. Data are shown in Fig. 2. Additional data include spring water of Grøndalen from 1926 (Orvin, 1944) and 2018 (this study), snow from 2016-2018 and river and tributary water of the Grøn River (Skakun et al., in review).**

| **Material** | | **core#9 unit I** | **core#9 unit II** | **core#9 unit III** | **core#9 unit IV** | **core#9 all units** | **Grøn River** | **Snow** | **Spring 1926** | **Spring 2018** |
|---|---|---|---|---|---|---|---|---|---|---|
| Core depth | [m bs] | 1.5-9.8 | 9.8-16.1 | 16.1-20.8 | 20.8-22.2 | 1.5-22.2 | surface | surface | surface | surface |
| n | | 16 | 7 | 8 | 3 | 34 | 1 | 1 | 1 | 1 |
| pH min-max | | 6.6-7.9 | 7.0-8.8 | 7.8-8.9 | 7.7-7.9 | 6.6-8.9 | -- | -- | -- | -- |
| pH mean | | 7.2±0.4 | 7.8±0.7 | 8.4±0.4 | 7.8±0.1 | 7.7±0.7 | 7.4 | 7.7 | -- | 8.8 |
| EC min-max | [µS $cm^{-1}$] | 5-106 | 27-269 | 133-834 | 100-108 | 5-834 | -- | -- | -- | -- |
| EC mean | [µS $cm^{-1}$] | 44±30 | 141±118 | 394±265 | 104±5 | 152±197 | -- | -- | -- | 1834 |
| ion content min-max | [mg $l^{-1}$] | 2.6-54.2 | 13.8-137.9 | 68.1-427.7 | 51.0-55.6 | 2.6-427.7 | -- | -- | -- | -- |
| ion content mean | [mg $l^{-1}$] | 22.3±14.9 | 72.2±60.5 | 202.0±136.0 | 53.3±2.3 | 77.8±100.9 | 118.4 | 16.4 | 879.2 | 1192 |
| $Na^+$ min-max | [mg $l^{-1}$] | 0.0-23.8 | 5.4-70.3 | 39.8-216.9 | 25.6-28.4 | 0.0-216.9 | -- | -- | -- | -- |
| $Na^+$ mean | [mg $l^{-1}$] | 8.2±6.8 | 30.8±25.2 | 107.3±68.1 | 27.2±1.5 | 37.8±52.3 | 7.6 | 5.3 | 333.3 | -- |
| $K^+$ min-max | [mg $l^{-1}$] | 1.7-4.1 | 0.3-2.1 | 0.2-2.8 | 0.2-0.3 | 0.2-4.1 | -- | -- | -- | -- |
| $K^+$ mean | [mg $l^{-1}$] | 2.5±0.7 | 1.1±0.7 | 1.1±1.0 | 0.3±0.1 | 1.7±1.1 | 0.9 | < 0.25 | 16.5 | -- |
| $Ca^{2+}$ min-max | [mg $l^{-1}$] | 0.0-0.5 | 0.0-0.2 | -- | -- | 0.0-0.5 | -- | -- | -- | -- |
| $Ca^{2+}$ mean | [mg $l^{-1}$] | -- | -- | -- | -- | -- | 13.0 | 0.3 | 4.9 | -- |
| $Mg^{2+}$ min-max | [mg $l^{-1}$] | -- | -- | 0.0-1.9 | -- | 0.0-1.9 | -- | -- | -- | -- |
| $Mg^{2+}$ mean | [mg $l^{-1}$] | -- | -- | -- | -- | -- | 9.1 | 0.3 | 6.1 | -- |
| $Cl^-$ min-max | [mg $l^{-1}$] | 1.1-14.4 | 4.3-25.1 | 14.3-120.7 | 8.8-12.4 | 1.1-120.7 | -- | -- | -- | -- |
| $Cl^-$ mean | [mg $l^{-1}$] | 6.4±4.1 | 12.2±7.8 | 51.1±40.3 | 11.0±1.9 | 18.5±26.6 | 5.3 | 8.0 | 113.5 | 15.3 |
| $SO_4^{2-}$ min-max | [mg $l^{-1}$] | 0.6-1.8 | 0.7-4.4 | 1.4-3.1 | 1.3-1.8 | 0.6-4.4 | -- | -- | -- | -- |
| $SO_4^{2-}$ mean | [mg $l^{-1}$] | 0.9±0.3 | 1.8±1.3 | 2.1±0.6 | 1.5±0.3 | 1.4±0.9 | 63.3 | 0.6 | 3.3 | 3.8 |
| $HCO_3^{2-}$ min-max | [mg $l^{-1}$] | 1.0-39.9 | 6.9-110.1 | 56.4-336.3 | 39.5-42.5 | 1.0-336.3 | -- | -- | -- | -- |
| $HCO_3^{2-}$ mean | [mg $l^{-1}$] | 13.5±11.5 | 51.6±41.8 | 163.3±106.8 | 40.5±1.7 | 59.2±81.4 | 19.2 | 2.0 | 372.3 | -- |
| $NO_3^-$ min-max | [mg $l^{-1}$] | 0.7-1.1 | 0.5-0.7 | 0.5-2.1 | 0.6-0.7 | 0.5-2.1 | -- | -- | -- | -- |
| $NO_3^-$ mean | [mg $l^{-1}$] | 0.7±0.1 | 0.6±0.1 | 0.8±0.5 | 0.7±0.1 | 0.7±0.3 | -- | -- | -- | -- |
| Alkalinity | [mM] | -- | -- | -- | -- | -- | -- | -- | -- | 2.19 |

**Table 3: Hydrochemical composition of water extracts of the sedimentary cores #9, #10 and #11 given as minimum, mean, maximum values, standard deviations (std) per core. Data are shown in Fig. 4.**

| **Sedimentary water extract** | | **core #9** | **core #10** | **core #11** |
|---|---|---|---|---|
| Core depth | [m bs] | 22.55-24.9 | 0-11.9 | 0-5.0 |
| n | | 5 | 10 | 4 |
| pH min-max | | 9.2-9.9 | 6.7-7.9 | 6.9-7.6 |
| pH mean | | 9.6±0.2 | 7.3±0.5 | 7.2±0.3 |
| EC min-max | [µS $cm^{-1}$] | 1011-2670 | 22-436 | 14-176 |
| EC mean | [µS $cm^{-1}$] | 1796±818 | 199±120 | 75±71 |
| ion content min-max | [mg $l^{-1}$] | 505.0-1335.0 | 10.8-218.0 | 6.9-88.1 |
| ion content mean | [mg $l^{-1}$] | 897.8±408.8 | 99.6±60.0 | 37.5±35.6 |
| $Na^+$ min-max | [mg $l^{-1}$] | 429.2-861.6 | 3.9-81.1 | 2.5-10.3 |
| $Na^+$mean | [mg $l^{-1}$] | 625.9±204.4 | 46.4±28.1 | 8.0±3.7 |
| $K^+$ min-max | [mg $l^{-1}$] | 14.4-22.6 | 1.3-15.4 | 0.6-5.1 |
| $K^+$ mean | [mg $l^{-1}$] | 18.5±3.7 | 8.0±4.2 | 2.6±2.3 |
| $Ca^{2+}$ min-max | [mg $l^{-1}$] | -- | 0.6-49.0 | 1.0-15.7 |
| $Ca^{2+}$ mean | [mg $l^{-1}$] | -- | 22.2±17.0 | 6.2±8.2 |
| $Mg^{2+}$ min-max | [mg $l^{-1}$] | -- | 0.5-4.1 | 0.3-6.4 |
| $Mg^{2+}$ mean | [mg $l^{-1}$] | -- | 2.0±1.3 | 2.6±3.3 |
| $Cl^-$ min-max | [mg $l^{-1}$] | 107.0-397.2 | 0.0-31.6 | 0.8-2.4 |
| $Cl^-$ mean | [mg $l^{-1}$] | 216.0±144.7 | 15.6±10.4 | 1.6±0.7 |
| $SO_4^{2-}$ min-max | [mg $l^{-1}$] | 52.6-93.8 | 1.4-138.0 | 1.4-50.1 |
| $SO_4^{2-}$ mean | [mg $l^{-1}$] | 74.7±14.9 | 47.4±38.9 | 18.3±22.4 |
| $HCO_3^{2-}$ min-max | [mg $l^{-1}$] | 289.0-836.8 | 4.2-49.0 | 4.2-40.3 |
| $HCO_3^{2-}$ mean | [mg $l^{-1}$] | 522.9±227.5 | 22.2±17.0 | 15.7±16.6 |
| $NO_3^-$ min-max | [mg $l^{-1}$] | 0.6-0.9 | 0.1-0.4 | 0.1-0.3 |
| $NO_3^-$ mean | [mg $l^{-1}$] | 0.7±0.1 | 0.2±0.1 | 0.2±0.1 |

**Figures**

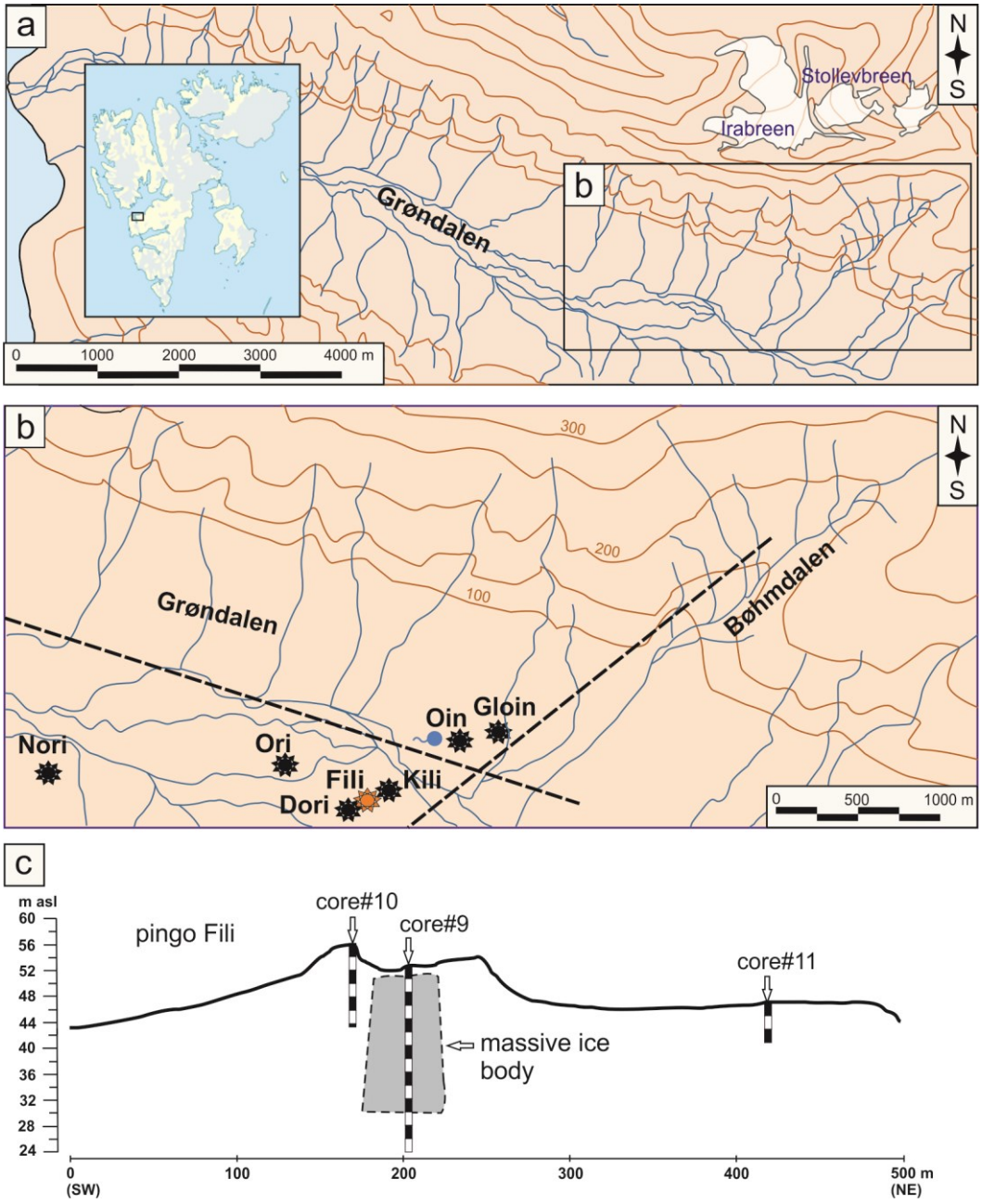


**Figure 1: Study region of Nordenskiöld Land on West Spitsbergen (inset), showing (a) the position of Grøndalen, (b) the position of seven pingos in Grøndalen (redrawn after https://toposvalbard.npolar.no), spring location (blue circle) and estimated faults locations (dotted lines) and (c) the drilling profile across Fili pingo (shown as orange star in b) with locations of cores #9, #10, ~~and~~ #11.**

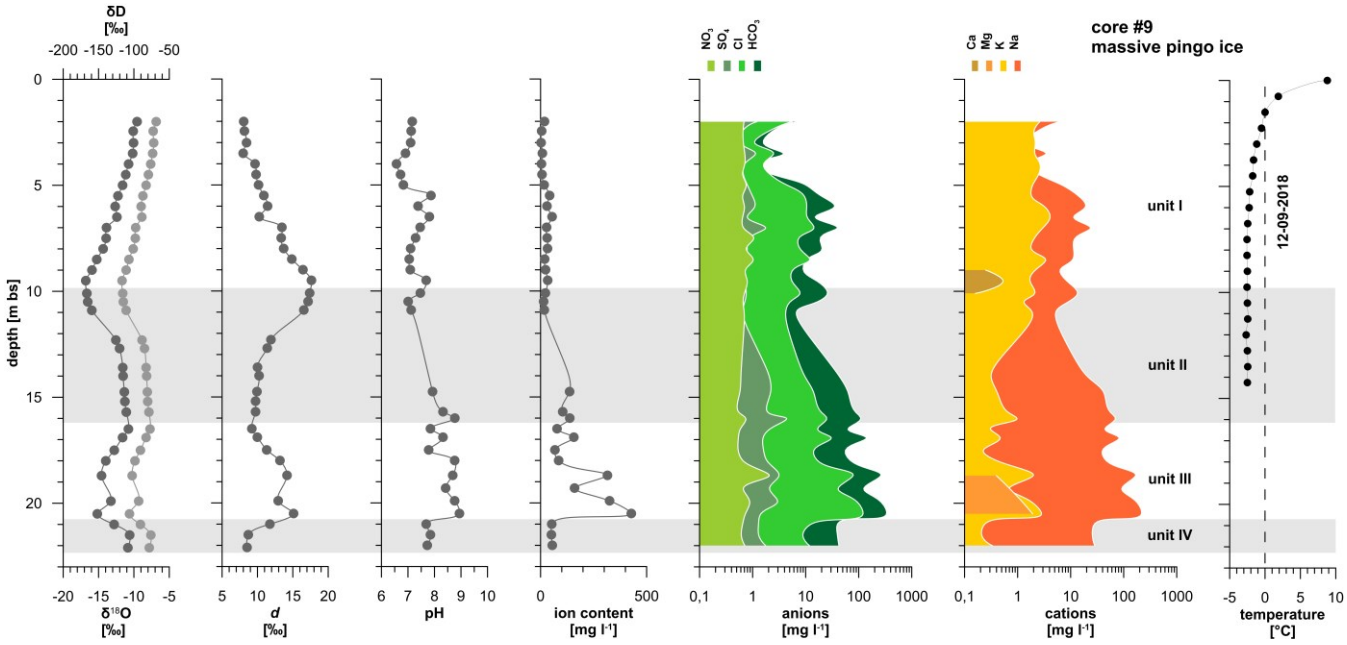


**Figure 2: Isotopic and hydrochemical composition of the massive ice of Fili pingo obtained from core#9 as well as thermometric data from the borehole on 12 September 2018. Light grey symbols in the first plot refer to the upper x-axis (δD). Data are given in Table 1 and Table 2.**

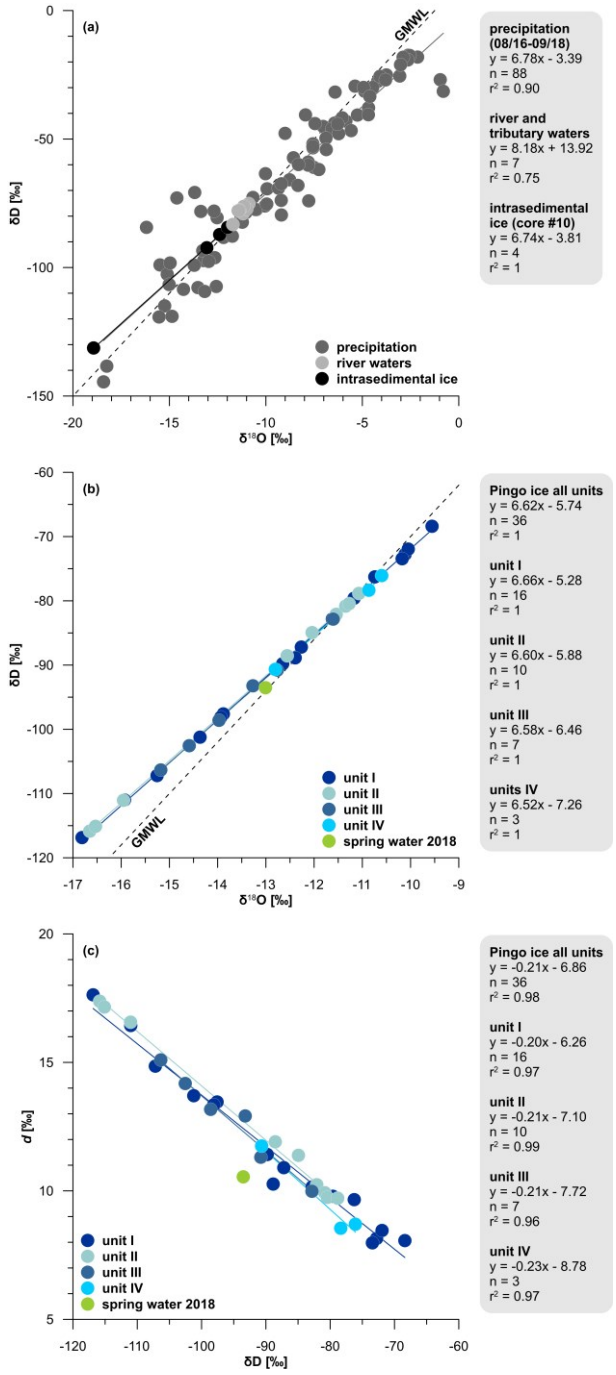


**Figure 3: Co-isotopic plots of (a) $\delta^{18}O$ and δD in modern precipitation (08/2016-09/2018) and water of the Grøn River and its tributaries (Shakun et al., in review), (b) $\delta^{18}O$ and δD in massive ice of core #9 from pingo and from spring water sampled, and (c) δD and deuterium excess (*d*) data in massive ice of core #9 from pingo and from spring water. Data are given in Table 1. Note different axis scales in (a) and (b).**

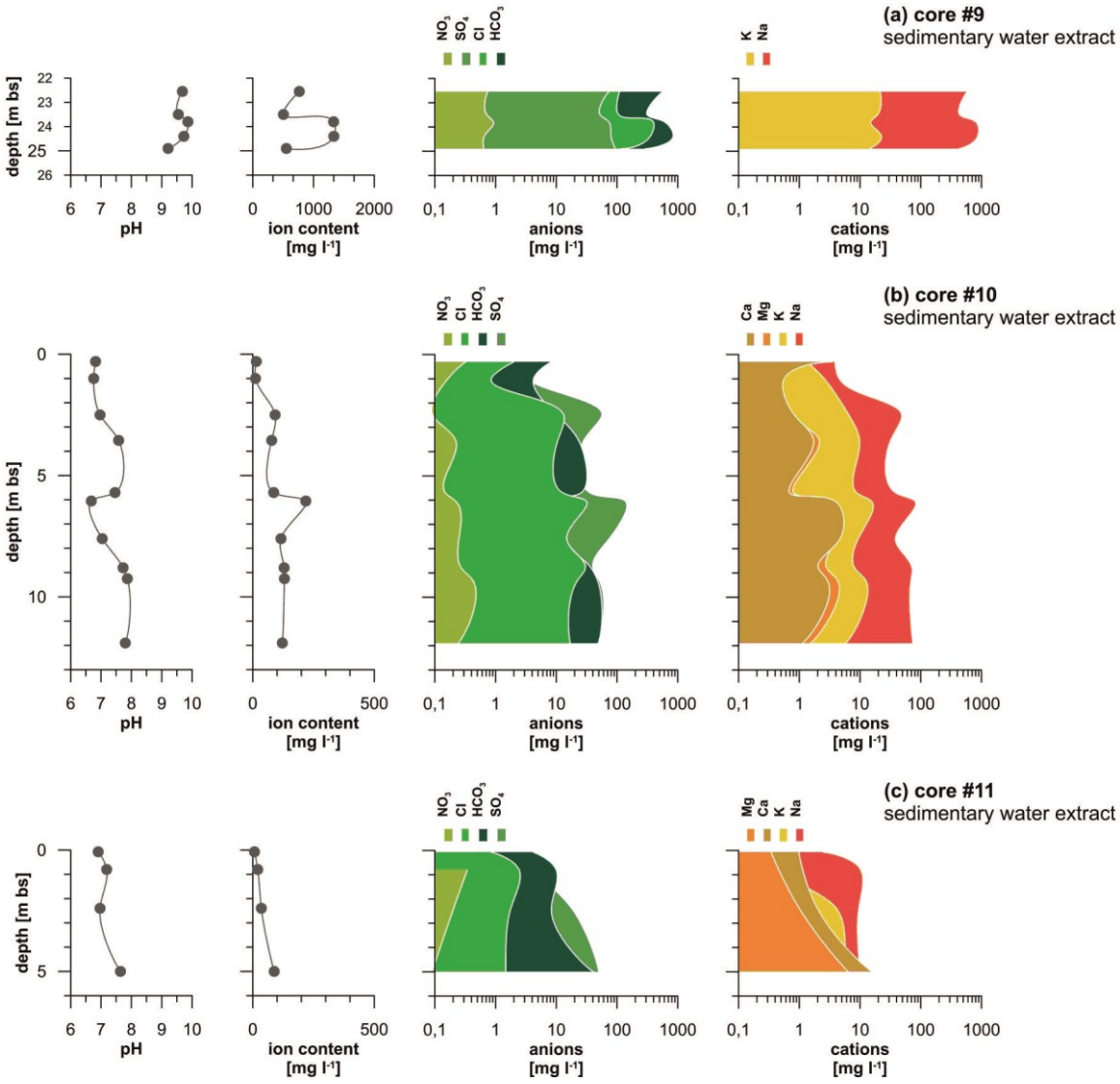


**Figure 4:Hydrochemical composition of water extracts from the sedimentary cores #9, #10 and #11. Data are given in Table 3. Note different axis scale for ion content in (a) reaching up to 1335 mg $l^{-1}$.**

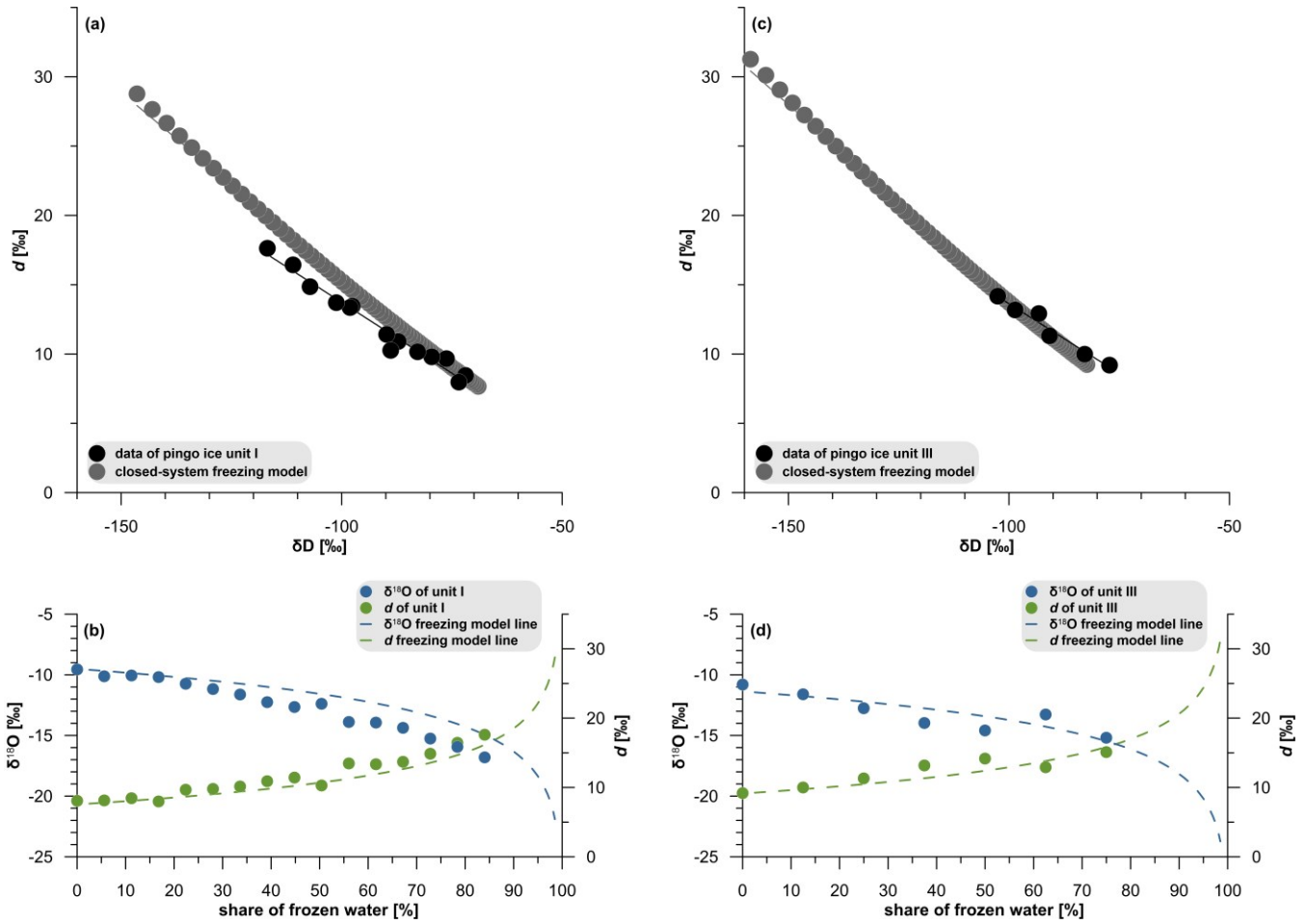


**Figure 5: Isotopic composition of unit I (a, b) and unit III (c, d) of the massive pingo ice of core #9 in comparison to freezing model data under closed-system conditions (Ekaykin et al., 2016).**

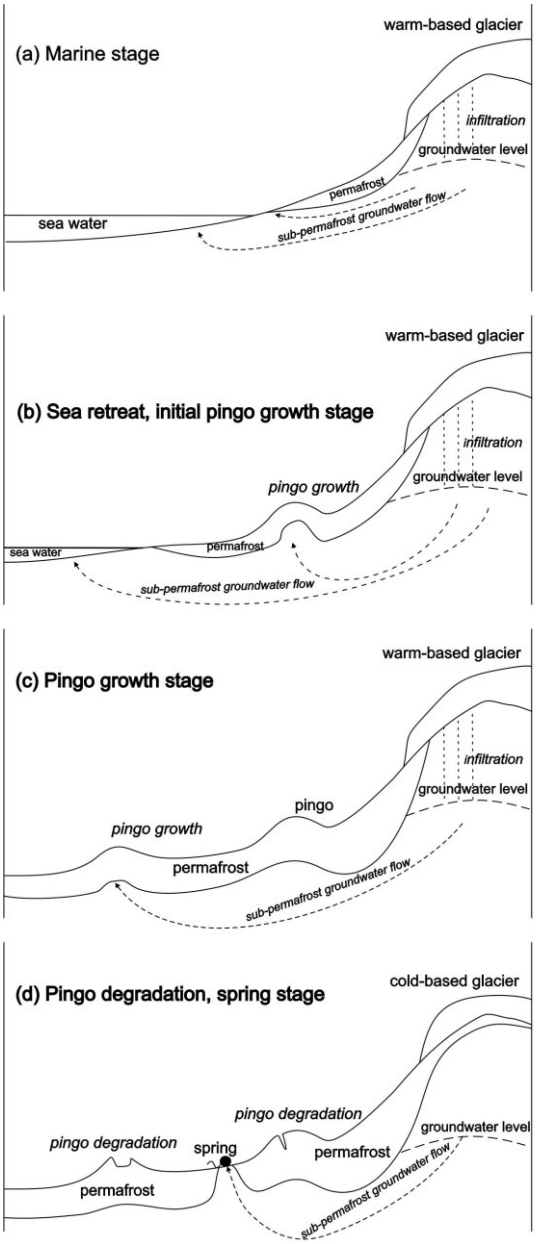


**Figure 6: Schematic sketch of Grøndalen evolution and pingo formation differentiating into (a) marine stage, (b) initial pingo growth after sea retreat and establishment of the valley's hydrological system, (c) continuing pingo growth along the topographic gradient and (d) current pingo degradation and occurrence of springs.**